Surface Potential Modelling of Hot Carrier Degradation in CMOS Technology

by

Kiraneswar Muthuseenu

A Thesis Presented in Partial Fulfilment
of the Requirements for the Degree
Master of Science

Approved April 2017 by the
Graduate Supervisory Committee:

Hugh Barnaby, Chair
Michael Kozicki
Yago Gonzalez Velo

ARIZONA STATE UNIVERSITY

May 2017

ABSTRACT

The scaling of transistors has numerous advantages such as increased memory density, less power consumption and better performance; but on the other hand, they also give rise to many reliability issues. One of the major reliability issue is the hot carrier injection and the effect it has on device degradation over time which causes serious circuit malfunctions.

Hot carrier injection has been studied from early 1980's and a lot of research has been done on the various hot carrier injection mechanisms and how the devices get damaged due to this effect. However, most of the existing hot carrier degradation models do not consider the physics involved in the degradation process and they just calculate the change in threshold voltage for different stress voltages and time. Based on this, an analytical expression is formulated that predicts the device lifetime.

This thesis starts by discussing various hot carrier injection mechanisms and the effects it has on the device. Studies have shown charges getting trapped in gate oxide and interface trap generation are two mechanisms for device degradation. How various device parameters get affected due to these traps is discussed here. The physics based models such as lucky hot electron model and substrate current model are presented and gives an idea how the gate current and substrate current can be related to hot carrier injection and density of traps created.

Devices are stressed under various voltages and from the experimental data obtained, the density of trapped charges and interface traps are calculated using mid-gap

technique. In this thesis, a simple analytical model based on substrate current is used to calculate the density of trapped charges in oxide and interface traps generated and it is a function of stress voltage and stress time. The model is verified against the data and the TCAD simulations. Finally, the analytical model is incorporated in a Verilog-A model and based on the surface potential method, the threshold voltage shift due to hot carrier stress is calculated.

DEDICATION

I dedicate this thesis to my ever-loving parents, friends, seniors and all the people who I have met in my life who have contributed for what I am now. A special thanks to my Dad (Appa), Mr. Muthuseenu and my Mom (Amma), Mrs. Suganthi who have worked so hard and sacrificed so much throughout their life with just one goal that their son should get what he wants.

ACKNOWLEDGMENTS

I would like to thank my adviser and mentor, Dr. Hugh Barnaby, who continues to guide and inspire me right from the time I started working with him. He closely watches every student working with him and knows their strength and weakness. In my case, having no prior work experience and being the youngest in the group, his constant motivation helps me to achieve my full potential in research work. I would also like to thank Dr. Michael Kozicki, who is a great researcher with vast knowledge, yet so simple and humble. After attending his classes, I learnt how to teach and make the classes interesting and I wish I can replicate the same when I become a Professor. I am also grateful to my other committee member Dr. Yago Gonzalez Velo for constantly checking my research work and motivating me.

I want to thank Dr. Ivan Sanchez Esqueda for providing the data required for my thesis and for clarifying the doubts I encountered. I would like to thank all my group members, especially Ian Livingston, Jennifer Taggart, Adnan Mahmud and Jeremy who helped me at various times by providing valuable advice both in research aspect and in personal aspect.

I would like to thank my parents for their love and support and it is only because of their hard-work I am able to pursue my dreams and achieve it. I am so grateful to two of my seniors, Dr. Ganesh Subramanian and Srinivasa Varadan Ramanujam, for guiding me after I came to USA. I also like to thank my friends and relatives for being there whenever I needed any support.

I want to express my gratitude to School of Electrical, Computer and Energy Engineering, Arizona State University and United States of America for providing me this opportunity. Last but not the least, I am so much thankful to my country India which has provided me everything I wanted in my life.

TABLE OF CONTENTS

Page

TABLE OF CONTENTS vi

LIST OF TABLES ix

LIST OF FIGURES x

CHAPTER

1 INTRODUCTION 1

1.1 Motivation 1

1.2 Hot Carrier Injection 3

1.3 Hot Carrier Injection Mechanisms 5

1.3.1 The Drain Avalanche Hot Carrier Injection (DAHC) 5

1.3.2 The Channel Hot Electron Injection (CHE) 7

1.3.3 The Substrate Hot Electron Injection (SHE) 7

1.3.4 The Secondary Generated Hot Electron Injection (SGHE) 8

1.4 Thesis Outline 9

2 HOT CARRIER DEGRADATION IN N-CHANNEL MOSFET 11

2.1 Introduction 11

2.2 Carrier Injection and Gate Current 11

2.3 Interface Trap Generation 14

2.3.1 Interface States ... 14

2.3.2 Interface Trap Generation Due to Hot Carriers ... 17

2.4 Effects of Hot Carrier Injection on Device Parameters ... 19

2.4.1 Hot Carrier Effect on the Threshold Voltage ... 19

2.4.2 Hot Carrier Effect on the Subthreshold Slope ... 20

2.4.3 Hot Carrier Effect on the Mobility ... 22

2.4.4 Hot Carrier Effect on the Transconductance ... 23

2.5 Hot Carrier Degradation in Long Channel MOSFET ... 23

2.5.1 Location of Defects ... 24

2.5.2 Problems Caused Due to Defect Localization in Measuring Degradation Parameters ... 26

2.5.3 Two-Piece Model ... 27

3 HOT CARRIER INJECTION MODELS ... 29

3.1 Introduction ... 29

3.2 Lucky Electron Model ... 30

3.3 Substrate Current Modelling ... 34

3.3.1 Origin of Substrate Current ... 35

3.3.2 Substrate Current Model Based on Lucky Electron Model ... 37

CHAPTER Page

4 ANALYTICAL MODEL FOR HOT CARRIER DEGRADATION 40

4.1 Introduction 40

4.2 Derivation of Analytical Model 40

4.3 Model Parameterization and Validation 44

4.3.1 Charge Separation Technique 45

4.3.2 Extraction of Fixed Charge and Interface Trap Density from the Data 49

4.3.3 TCAD Validation 53

4.4 Incorporating the Analytical Model Using Surface Potential Method 56

5 CONCLUSION 59

REFERENCES 61

LIST OF TABLES

Table Page

1.1 Energy of the Carriers and the Mechanisms Involved Causing Device Degradation... 4

4.1 Each Device's Doping Concentration, Oxide Thickness and the Voltage at Which They Are Stressed ... 50

4.2 Mid-gap Current and Threshold Voltage Current for Different Device and the Corresponding Mid-gap Voltage and Threshold Voltage for Pre-stress and Post-stress Condition... 51

4.3 Density of Trapped Oxide Charges and Interface Traps Generated for Different Stress Voltage ... 52

4.4 Density of Traps Calculated Using Analytical Model and from the Data ... 54

LIST OF FIGURES

Figure Page

1.1 Doubling of Transistors Vs Years (Moore's Law) 1

1.2 N-channel MOSFET Showing Hot Carrier Injection 3

1.3 Energy Band Diagram Showing Barrier Height for Electron and Hole Injection from Silicon to Gate Oxide... 5

1.4 Drain Avalanche Hot Carrier Injection Mechanism 6

1.5 Channel Hot Electron Injection Mechanism.. 7

1.6 Substrate Hot Electron Injection Mechanism 8

1.7 Secondary Hot Electron Injection Mechanism 9

2.1 Carrier Injection and Gate Current Vs Gate Bias 12

2.2 Relationship Between Interface States and Gate Bias at Different conditions (a) Flatband, (b) Accumulation, (c) Depletion, (d) Mid-gap, (e) Inversion........................... 16

2.3 Plot Showing Increase in Threshold Voltage Due to Hot Carrier Effect.................... 20

2.4 Plot Showing Increase in Subthreshold Swing Due to Hot Carrier Effect 21

2.5 Plot Showing the decrease in Subthreshold Slope Due to Hot Carrier Effect............ 22

2.6 Plot Showing Decrease in Transconductance Due to Hot Carrier Effect 23

2.7 Normal and Reverse Mode Drain Current Vs Drain Bias Measured Before and After Hot Carrier Stress in NMOSFET... 25

2.8 Schematic of Two Transistor Model... 27

2.9 Channel Conductance Vs Gate Voltage.. 28

3.1 Schematic Showing Transverse Band Diagram in NMOSFET 31

Figure Page

3.2 Scattering Events Associated With Lucky Hot Electron Model 31

3.3 The Probabilities Associated With Lucky Hot Electron Model 32

3.4 Plot Showing Substrate Current Vs Gate Bias for Different Drain Bias 36

3.5 Plot Showing Decrease in Lateral Electric Field as Gate Bias Increased 37

4.1 Carrier Multiplication Due to Impact Ionization 41

4.2 Plot Showing Log Drain Current Vs Gate Voltage and Mid-gap Current and Threshold Voltage Current 49

4.3 Plot Showing Pre-stress and Post-stress of Both Data and TCAD Simulation With Density of Traps Value Obtained Using Mid-gap Voltage Method 53

4.4 Plots Comparing Post-stress Condition Between Analytical Method and Data 55

4.5 Plot Comparing N_{ot} Calculated Using Analytical Model and Using Data 55

4.6 Plot Comparing N_{it} Calculated Using Analytical Model and Using Data 56

1 INTRODUCTION

1.1 Motivation

Moore predicted that the number of transistors in an integrated circuit will approximately be doubled for every two years as shown in the Fig. 1.1 [1]. This law has been the driving force for innovation in semiconductor industries for more than 5 decades. According to ITRS, device cost and performance will be strongly correlated to dimensional and functional scaling of CMOS since information technology allows the semiconductor industry to expand into a wide range of new applications [2].

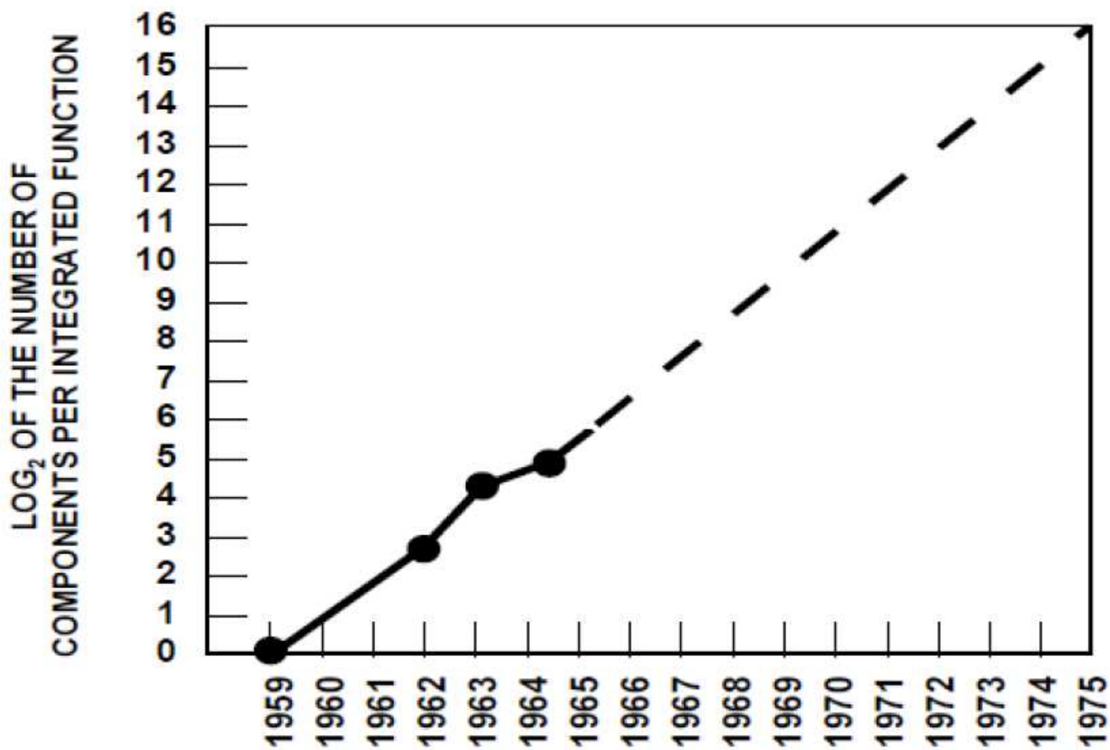

Figure 1.1 Doubling of Transistors Vs Years (Moore's Law) [1]

At present, microprocessors have more than a billion transistors and this has led to improved capabilities in processing speed, power and memory capacity [2]. However, a logical choice of keeping the internal electric fields constant with device scaling had to be abandoned due to some disadvantages associated with it such as [3], [4]:

- Compatibility with power supply is lost.
- The threshold voltage and the subthreshold slope of the device will not be scaled, thereby causing a decrease in noise margin.
- The parasitic capacitance will not be scaled and this leads to reduced operating speed in advanced technologies.

In the alternative scheme of constant voltage scaling, electric fields increase with device scaling. This results in increased carrier velocities and hence higher operating speed. However after a certain critical field value, instead of having positive effect on device performance, they cause mobile carriers to attain relatively high energies[5]. This causes many reliability issues[6], [7], [8] in the device through a variety of mechanisms [4].One of the major reliability issues among them is the injection of energetic carriers into the gate oxide which is called hot carrier injection [9], [10]. The importance of the hot carrier injection is that it damages the gate oxide permanently through carrier trapping and interface trap generation, which causes shift in device parameters such as, threshold voltage, subthreshold slope, and transconductance [11], [12]. This is called hot carrier induced degradation in MOSFETs [13].

1.2 Hot Carrier Injection

In this section, an overview of the hot carrier injection phenomenon is provided. As the MOSFET features are being scaled down, the operating voltages are also reduced but the scaling factor for voltage is less than that of device dimension scaling and so the hot carrier injection is more an important consideration in sub-micron technologies. The large voltage drop across the pinch off region results in a high lateral electric field close to the drain region. Therefore, the carriers travelling from the source to drain gain significant kinetic energy in this high field region and those carriers with energy higher than that of the equilibrium thermal energy are called hot carriers [9], [10].

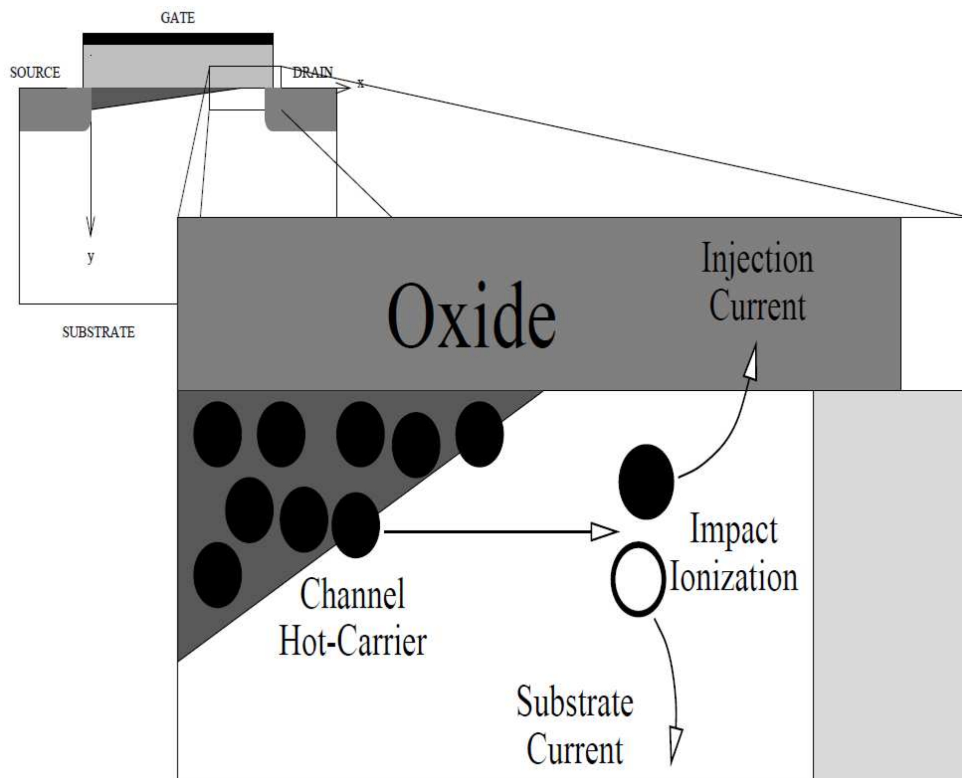

Figure 1.2 N-channel MOSFET Showing Hot Carrier Injection [14]

Carrier Energy (E)	Mechanism	Effect on Device Performance
1.3 eV < E < 1.8 eV	Impact Ionization	Snap-back, device breakdown, avalanche effect and latch up
E > 3.2 eV	Hot electron injection	Shift in device parameters due charge trapping in gate oxide and interface trap generation
E > 4.8 eV	Hot hole injection	

Table 1.1 Energy of the Carriers and the Mechanisms Involved Causing Device Degradation

When the energy of hot carriers is greater than impact ionization threshold (1.6 eV) [4], they create electron-hole pairs near the drain. When these carriers have energies higher than the potential barrier between Si and SiO2 with their momentum also directed towards the Si-SiO2 interface, they get injected into the gate oxide [5], [13]. A portion of the carriers that are injected into the gate oxide reaches the gate terminal, thus contributing to gate current. However, some of the remaining injected carriers get trapped at certain defects present in the gate oxide [15], [16] and in addition, they also result in the increase in interface trap density present at the Si-SiO2 interface [17], [18], [19]. These new defects in the gate-oxide and at the Si-SiO2 interface cause changes to mobility, surface potential and other device parameters which affect the lifetime of MOSFET's [10]. As shown in Fig. 2, the energy barrier for injection of electrons (3.1eV) is considerably smaller than that for holes (4.8eV) making hole-injection a less probable event as compared to electron-injection and thus the degradation is more severe in NMOS [20], [14].

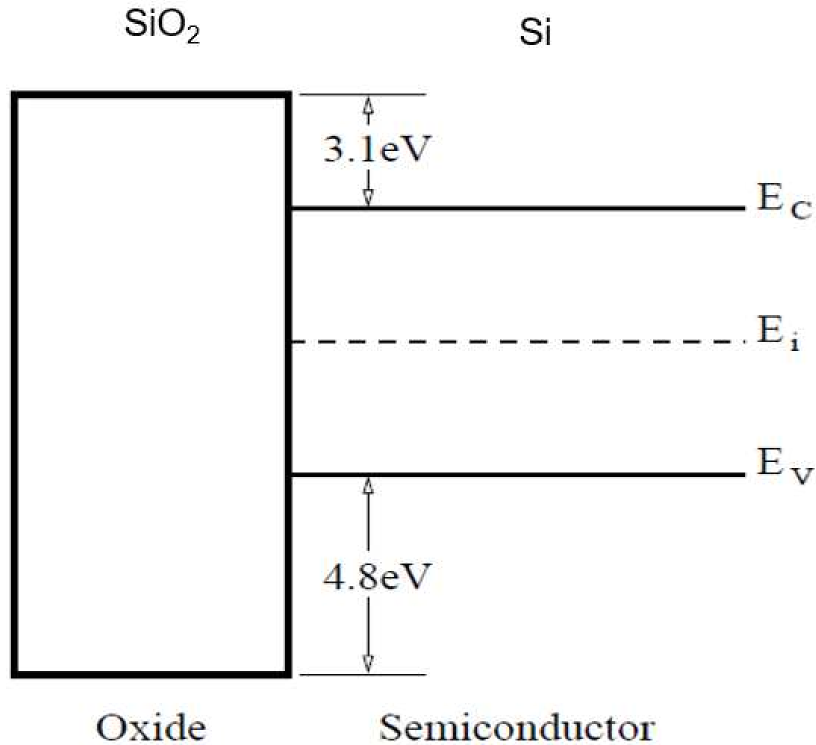

Figure 1.3 Energy Band Diagram Showing Barrier Height for Electron and Hole Injection from Silicon to Gate Oxide [14]

1.3 Hot Carrier Injection Mechanisms

When MOSFETs function under high electric fields, the mobile carriers in the channel can attain high energies and result in incorrect circuit operation. The instabilities of MOSFET parameters with operation time have been studied for a long time, and it has been found out that many of these instabilities are due to the damage caused by hot carrier injection to the gate oxide of MOSFET [21], [22], [23]. There are four types of hot carrier injection mechanisms.

1.3.1 The Drain Avalanche Hot Carrier Injection (DAHC)

The drain avalanche hot carrier injection causes the worst device degradation at room temperature. When the MOSFET is operated in the saturation region, that is when

the voltage applied at the drain terminal is higher than that of the gate terminal, the carriers in the channel gain high kinetic energy in the pinch off region and reach the drain terminal. These high-energy carriers undergo impact ionization near the drain terminal and thereby, create some electron hole pairs. Some of the generated electrons gain enough energy to overcome the electric potential barrier between the gate oxide and the silicon substrate and get injected into the gate oxide. These injected hot carriers sometimes get trapped within the oxide and create a fixed space charge which causes change in device parameters such as threshold voltage. As the operation time of the device increases, more charges get trapped and passivated traps at the interface get de-passivated (interface traps), and this causes further degradation in device parameters. Meanwhile, most of the holes generated by impact ionization flow back to the substrate and contributes to a large portion of the substrate current [9].

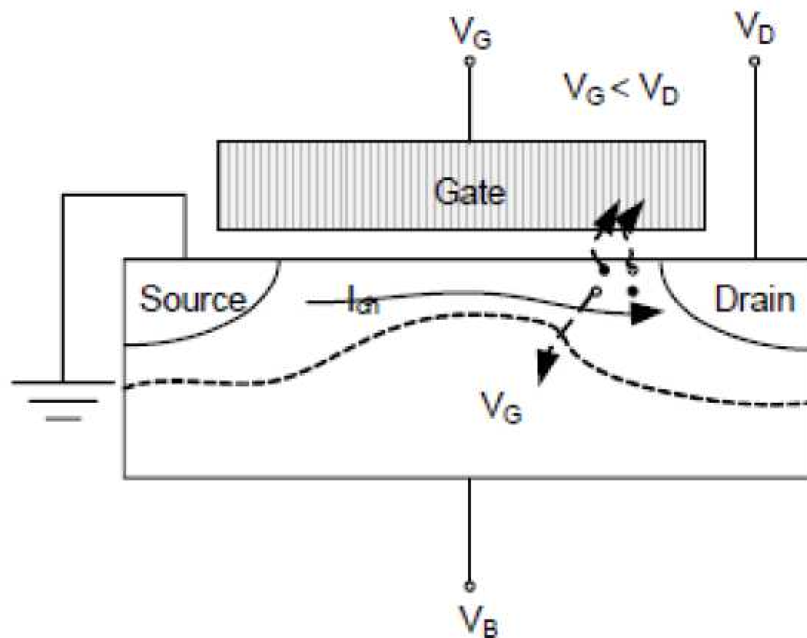

Figure 1.4 Drain Avalanche Hot Carrier Injection Mechanism [24]

1.3.2 The Channel Hot Electron Injection (CHE)

Channel hot electron injection happens when both the gate voltage and drain voltage are higher than the source voltage and drain voltage is approximately equal to gate voltage [9]. As the carriers in the channel flow towards the drain, they gain energy and some of them get scattered and diverted towards the gate oxide. If these diverted carriers have enough energy to overcome the oxide-silicon potential barrier, then they get injected into the gate oxide. A part of these injected carriers stay inside the gate oxide permanently and affect the electrical characteristics of the MOSFET and the remaining carriers reach the gate terminal and causes gate current Ig.

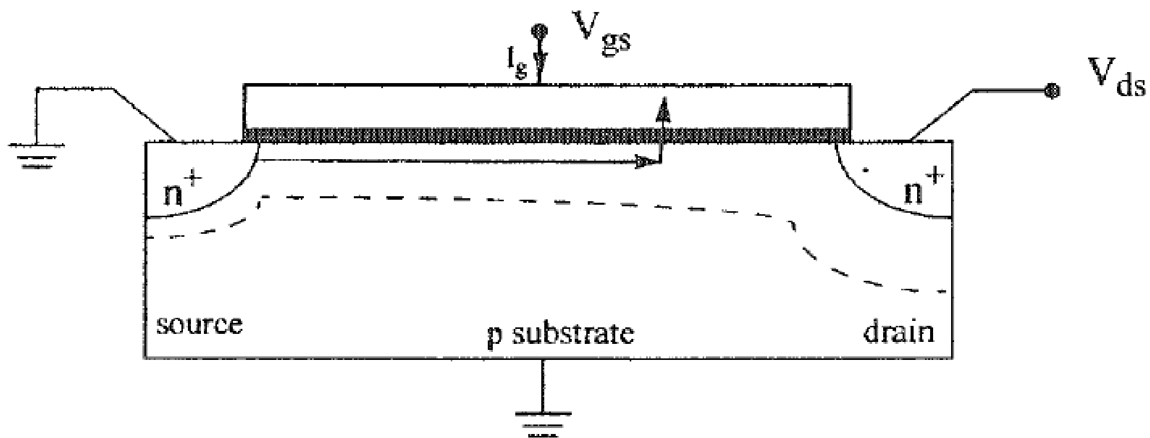

Figure 1.5 Channel Hot Electron Injection Mechanism [25]

1.3.3 The Substrate Hot Electron Injection (SHE)

When a strong electric field exists between the gate and the substrate, the electrons, which are generated in the substrate due to thermal electron-hole pair generation, will get accelerated towards the gate oxide [9]. If these accelerated electrons have enough energy to cross the potential barrier, then they get injected into the gate oxide. This mechanism of

hot-electron injection is not a major problem in short channel devices when compared with long channel devices because most of the electrons are absorbed into the source and drain regions of the device and only a small fraction of them reach the gate oxide.

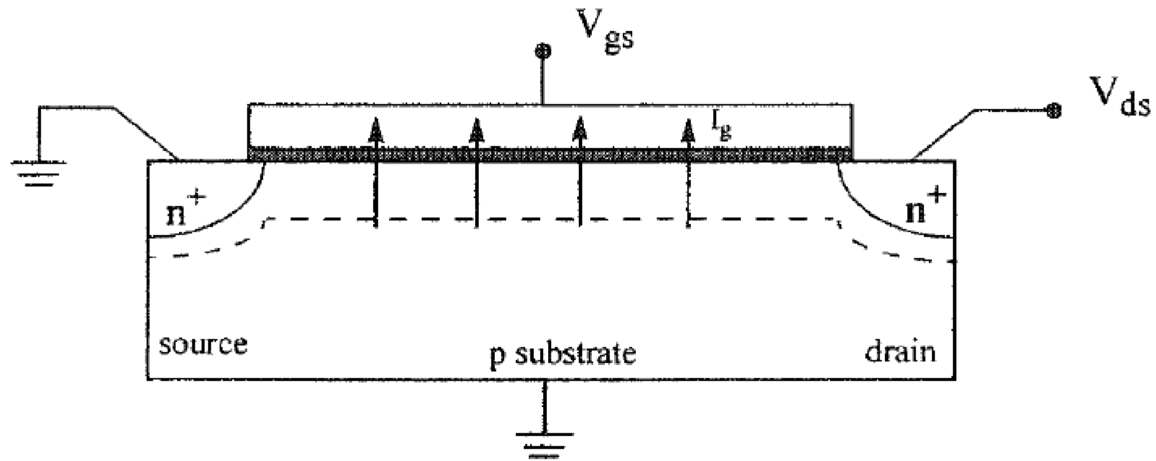

Figure 1.6 Substrate Hot Electron Injection Mechanism [25]

1.3.4 The Secondary Generated Hot Electron Injection (SGHE)

Secondary generated hot electron injection involves the generation of hot carriers from impact ionization involving a secondary carrier which was created by an earlier incident of impact ionization [9]. When a high voltage is applied at the drain terminal, it results in a field which tends to drive the hot carriers generated by the secondary carriers to the surface region. If these carriers are able to overcome the oxide-silicon potential barrier, they get injected into the gate oxide.

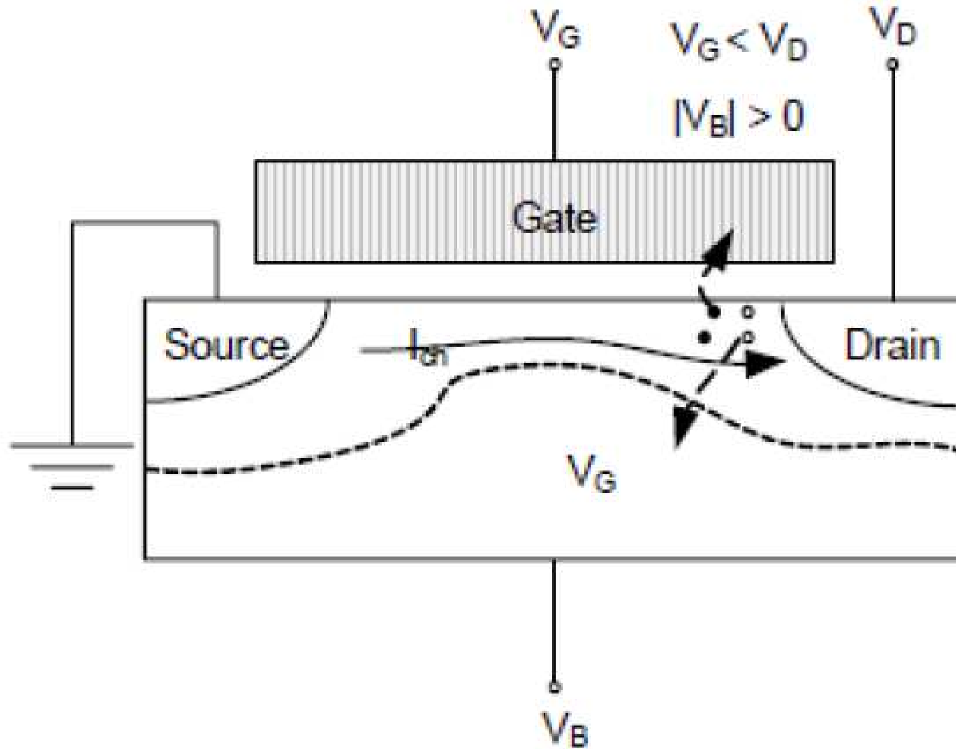

Figure 1.7 Secondary Hot Electron Injection Mechanism [24]

1.4 Thesis Outline

Most of the existing degradation models for hot carrier injection are based on the calculation of total threshold shift and thus predicting the device lifetime. In this thesis, the two components involved in threshold shift namely, oxide trapped charges and interface traps are calculated separately and a model calculating the density of these traps as a function of stress voltage and time is presented.

In the chapter 1, a brief introduction about the hot carrier injection and various mechanisms through which injection of hot carriers into the gate oxide happens is presented. Chapter 2 of the thesis includes two main sections, the first part deals with the effect of hot carrier injection namely generation of interface traps and trapped charges in

the oxide and the second part is about the effect of these traps on the device parameters and how it varies based on the channel length of the MOSFET. The two widely used physics-based hot carrier injection models, lucky hot electron gate current model and substrate current model is discussed in chapter 3. In chapter 4, a simple analytical model which is based on the substrate current model is used to calculate the density of oxide trap charges and interface traps which are created due to hot carrier injection is presented. Then the parameters present in the analytical model are calculated using the experimental data and the validation of the model is done using TCAD simulations. Finally, the model is incorporated in the Verilog-A, where the threshold voltage shift due to the traps are calculated using surface potential method and this can be used for circuit simulations. Chapter 5 summarizes the work done in this thesis and provides the possible future work that can be done.

2 HOT CARRIER DEGRADATION IN N-CHANNEL MOSFET

2.1 Introduction

Hot carrier degradation in NMOS has been studied for more than 20 years and considerable progress has been made in understanding hot carrier injection in long channel devices [13], [26], [27], [28], [29]. However, as the technologies evolved and device dimensions reduced, the theories based on long channel devices were not enough to explain the device response due to HCI because, the energy of hot carriers can drastically change based on the supply voltage. Based on the hot carrier energy, different physical processes such as carrier injection into the oxide, charge trapping, impact ionization and interface trap creation can be present and their contribution to degradation also varies [30], [31], [32]. Therefore, it is necessary to understand the bias dependences of these process and this chapter provides the summary of these process involved during hot carrier degradation in NMOS.

2.2 Carrier Injection and Gate Current

The main cause for hot carrier degradation is due to injection of hot carriers from the channel into the gate oxide. The injection of carriers at any given location along the channel is determined by two factors, the concentration of the carriers in the channel and the electric field at that point of injection [33], [14].

In the subthreshold region, the injection of carriers into gate oxide is negligible because the concentration of carriers in the channel is very low. As the gate bias increases,

the concentration of the carriers in the channel increases and thus the electron and hole injection current increases.

However, there is always a point of discussion in hot carrier literature whether it is hot electrons or hot holes responsible for device degradation. It is argued that if holes were responsible for degradation, then threshold voltage shift in PMOS will be much greater than in NMOS because PMOS channel is inverted and will be filled with holes; but even at higher stress voltage, PMOS degradation was less than that of NMOS. Therefore, it was understood that hot electron injection was more significant than hot hole injection [5].

The relation between injection current, gate current and trapped carriers in a NMOSFET as a function of gate bias is shown in the figure and is explained below [13].

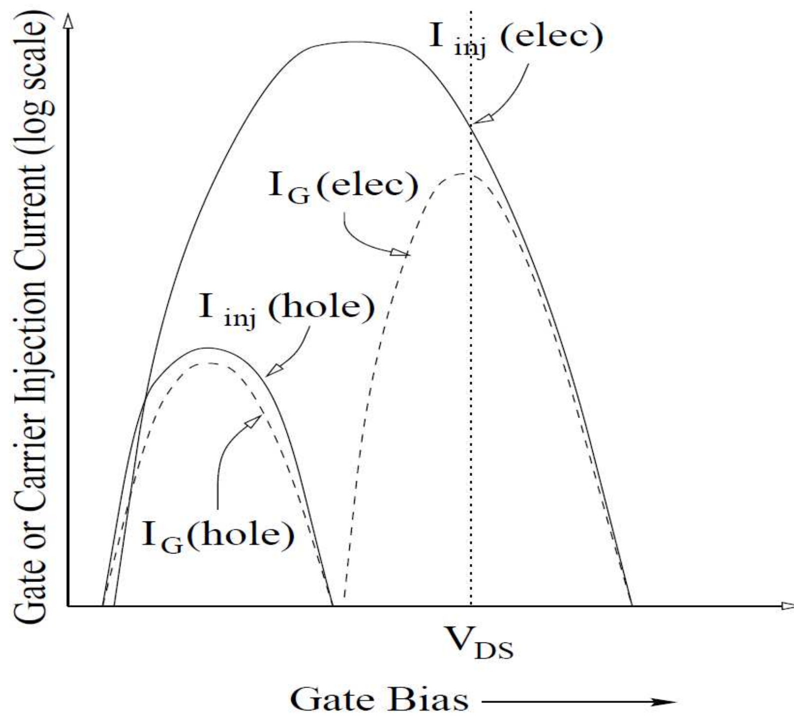

Figure 2.1 Carrier Injection and Gate Current Vs Gate Bias [14]

At low gate voltage, the transverse electric field and the Schottky barrier lowering favors the hole injection into the oxide more than electron injection and since the oxide field also favors the transport of injected holes, most of them reach the gate terminal. Thus at low gate bias, gate current is primarily due injected holes [26], [27].

As the gate bias increases, the Schottky barrier lowering decreases and the electron injection current increases due to relatively smaller potential barrier for electrons at oxide-silicon interface. However, the field in the oxide is against the electron transport and thus most of the injected electrons either scatter back to the interface or gets trapped in the oxide. Therefore at this bias condition, the gate current is low when compared with electron injection current.

As gate bias is increased, the opposing oxide field decreases and a larger proportion of injected electrons contribute to the gate current and thus the gate current peaks when $V_{GS}=V_{DS}$.

When $V_{GS} > V_{DS}$, the lateral electric field decreases causing the electron injection also to decrease, but the oxide field favors the electron transport to the gate terminal and thus gate current is almost equal to electron injection current.

Some of the important characteristics of the gate and injection current in NMOS are [14]:

- Electrons are injected into gate oxide under all gate bias.
- The peak of the hole injection current is smaller than that of the electron injection current because the oxide-silicon barrier is large for hole injection.

- The amount of holes getting trapped in the oxide is negligible when compared with electrons, since most of the injected holes reach the gate terminal, whereas in the case of electrons, during the mid-bias region most of the injected electrons gets trapped in the oxide.

Therefore, it can be concluded that in NMOS, bulk oxide defect generation is due to hot electrons getting trapped in the gate oxide.

2.3 Interface Trap Generation

Various measurements of the MOSFETs subjected to hot carrier degradation have showed that besides charges getting trapped in the gate oxide, interface traps are also generated, and also, under some conditions interface traps are the main cause for device degradation [34], [35]. Hence an understanding of the interface states and its generation by hot carrier injected is required and is presented below.

2.3.1 Interface States

Interface states or interface traps are energy levels located at oxide-silicon interface that can capture or release electrons. They are created due to imperfections like lattice mismatch, disconnected chemical bonds or impurities [36]. They can be classified into two types: the interface state which is electrically neutral when occupied by an electron and positive when the electron is released is called a donor like interface trap, and an acceptor like interface state is the one which is electrically negative when occupied by electron and neutral when the electron is released [37]. It is generally assumed that donor like interface traps are located in the lower half of the bandgap while acceptor like interface traps are located in the upper half. As the position between energy level and Fermi level varies, the

occupation condition of that trap level also varies. Hence the electrical charge of an interface trap is a function of band bending and gate voltage [5], [37], [38], [39]. Figure 2.2 shows this dependency in a p-substrate MOS capacitor.

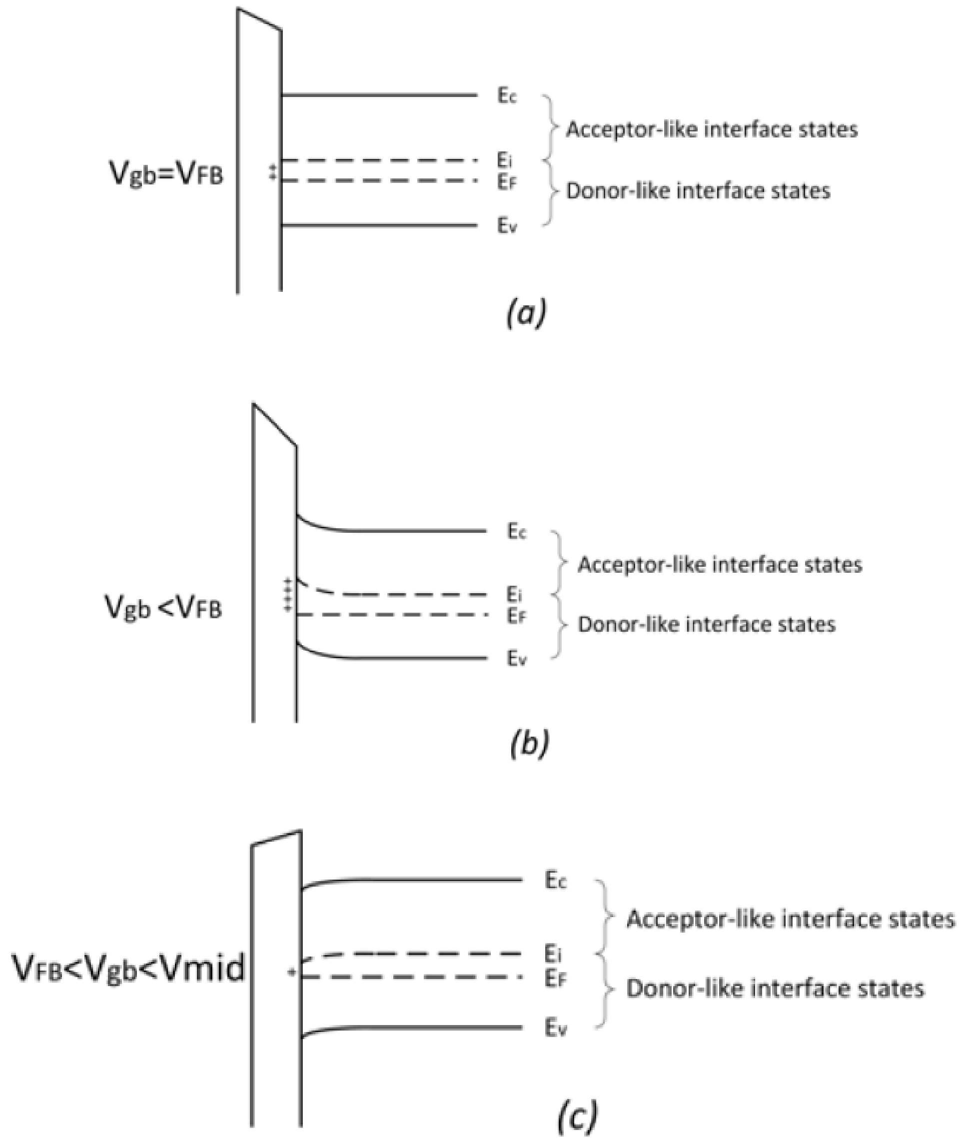

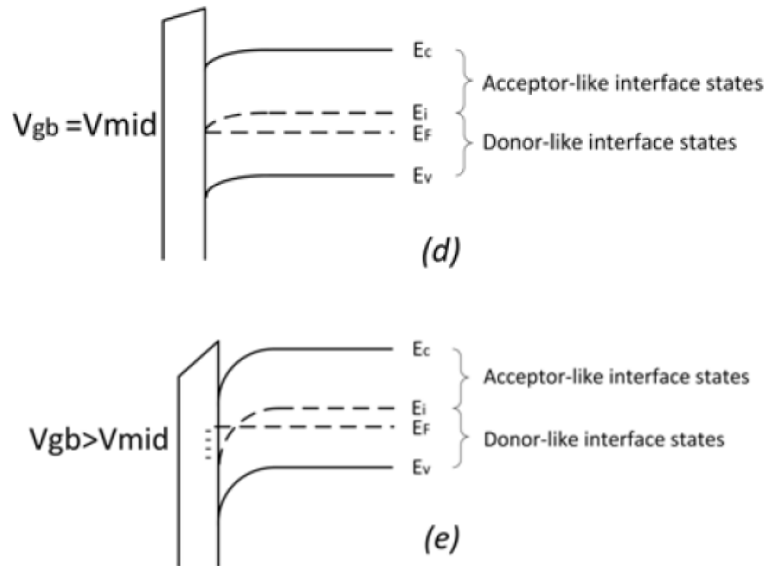

Figure 2.2 Relationship Between Interface States and Gate Bias at Different conditions (a) Flatband, (b) Accumulation, (c) Depletion, (d) Mid-gap, (e) Inversion [40]

V_{gb} is the voltage between the gate and substrate, V_{fb} is the flat band voltage and V_{mid} is the mid-gap voltage at which the intrinsic Fermi level (E_i) reaches the Fermi level (E_f).

Flatband:

When $V_{gb} = V_{fb}$, all the acceptor like interface traps are above E_f and hence they are electrically neutral. Donor like traps which are present below the Fermi level are neutral and which are present above the Fermi level are positive. Therefore, in the flatband condition, only donor like traps above the Fermi level contribute positive charge.

Accumulation:

When $V_{gb} < V_{fb}$, the bands bend up and so the acceptor type traps remain neutral, on the other hand donor like traps contribute more positive charges.

Depletion:

When $V_{fb} < V_{gb} < V_{mid}$, the band bends down but the acceptor type traps still remain neutral whereas donor like traps contribute less positive charge.

Mid-gap:

It is a transition point between the depletion and the inversion. As V_{gb} is increased and when $V_{gb} = V_{mid}$, E_i touches E_f and during which all interface states are neutral.

Inversion:

When $V_{gb} > V_{mid}$, parts of acceptor like traps below the Fermi level capture electron and produce negative charge. The other acceptor like traps and donor like traps remain neutral.

Therefore, based on the voltage applied between the gate and substrate the type and number of charges present at the oxide-silicon interface varies, contributing to shifts in threshold voltage, subthreshold slope and transconductance.

2.3.2 Interface Trap Generation Due to Hot Carriers

As seen from the above section, the injected hot carriers sometimes get trapped in the oxide causing device degradation and in addition to that hot carriers also create interface traps [13], [5], [41].

Electrons which have lighter effective mass when compared with holes will have longer mean free path and hence gain more energy and cause high impact ionization rate. Also, conduction band offset at the oxide-silicon interface is smaller than valence band

offset and hence electrons can create interface traps easily by injection over the oxide barrier [13].

For both PMOS and NMOS, the interface trap (NIT) density peaked at hole injection regimes and the lack of correlation between substrate current and NIT peak density was attributed to hot hole induced degradation and also holes were orders of magnitude more efficient for trap creation [41], [42], [43], [44].

On a related argument, it is still not very clear whether the carriers need to be injected into the oxide to generate defects. It was claimed that hot electron injection is necessary to create interface traps, in other words if the electron energy is less than the conduction band offset then there would be neither electron injection into the oxide nor the interface traps [13]. Therefore, if the supply voltage is less than 2.5V, hot carrier injection should be eliminated but the interface traps were created at biases even less than 0.9V [34], [35], [45]. Also, experiments were conducted by injecting hot electrons from the substrate into gate oxide and the interface trap density was measured [46]. When a gate bias is applied, hot electrons produced higher source and drain current but gate current was reduced drastically. Even in this condition, interface traps were created and hence it can be concluded that electron injection is not needed for interface trap creation. When the gate bias was reversed, the gate current and the degradation increased dramatically but the substrate current did not change [47]. This showed that when carrier injection takes place, interface trap density increases dramatically.

Therefore, following can be concluded from the above discussion [48]:

- Both the hot holes and hot electrons are responsible for interface trap creation.
- Interface trap density is maximum when hot hole injection is maximum and they are orders of magnitude more efficient than hot electrons.
- Hot carrier injection is not necessary to create interface traps but the density of interface traps increases dramatically when carrier injection takes place.

2.4 Effects of Hot Carrier Injection on Device Parameters

HCI degrades the device and affects the device parameters, such as threshold voltage, subthreshold swing, mobility and transconductance by introducing additional trapped charges and interface states inside the gate oxide [11], [12]. In this section, the relationship between HCI and these device parameters are discussed.

2.4.1 Hot Carrier Effect on the Threshold Voltage

The effect of additional trapped charges and acceptor like interface traps created during HCI on the threshold voltage can be given as

$$V_{Th} = 2\phi_B + \frac{\sqrt{2qN_A\epsilon_S(2\phi_B - V_{SB})}}{C_{OX}} + \phi_{MS} - \frac{Q_0}{C_{OX}} - \frac{Q_{IT}}{C_{OX}}, \qquad (2.1)$$

where, ϕ_B is the bulk potential,

N_A is the substrate doping concentration,

q is the electron charge,

ϵ_S is silicon permittivity,

ϕ_{MS} is metal semiconductor work function,

Q_0 is the density of trapped charges in gate oxide,

Q_{IT} is the density of interface trap charges,

C_{OX} is gate oxide capacitance.

Both the trapped charges (electrons) and interface traps (acceptor like at threshodl) are electrically negative and hence the threshold voltage of a degraded NMOS increases which can be seen in the figures below. It is a plot of data obtained from 28nm technology transistor stressed at 2V [36], [37].

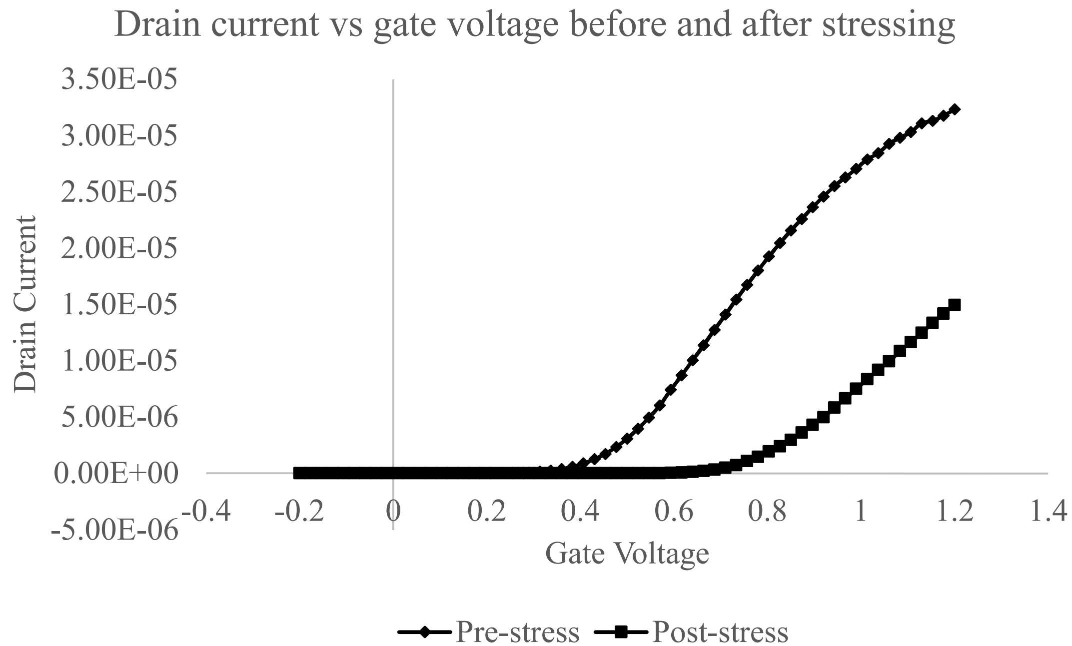

Figure 2.3 Plot Showing Increase in Threshold Voltage Due to Hot Carrier Effect

2.4.2 Hot Carrier Effect on the Subthreshold Slope

The subthreshold slope of a degraded device is affected only by the interface traps and not due to the trapped charges inside the gate oxide [37], [39]. This is because, the total

charge contribution by these trapped defects are fixed and independent of the applied bias, thereby causing only horizontal shift in the log Id versus Vg plot. A capacitance value proportional to the density of interface traps C_{IT} can be modelled based on the below equation,

$$S = \frac{(\ln 10)(V_t)(C_{OX} + C_{SC} + C_{IT})}{C_{OX}}, \quad (2.2)$$

where, S is subthreshold swing (or inverse sub-threshold slope),

V_t is the thermal voltage,

C_{SC} is the semiconductor capacitance,

C_{IT} is the capacitance due to interface states.

Subthreshold swing will increase during HCI since more interface traps are created which causes larger interface state capacitance. This can be observed in the figure below.

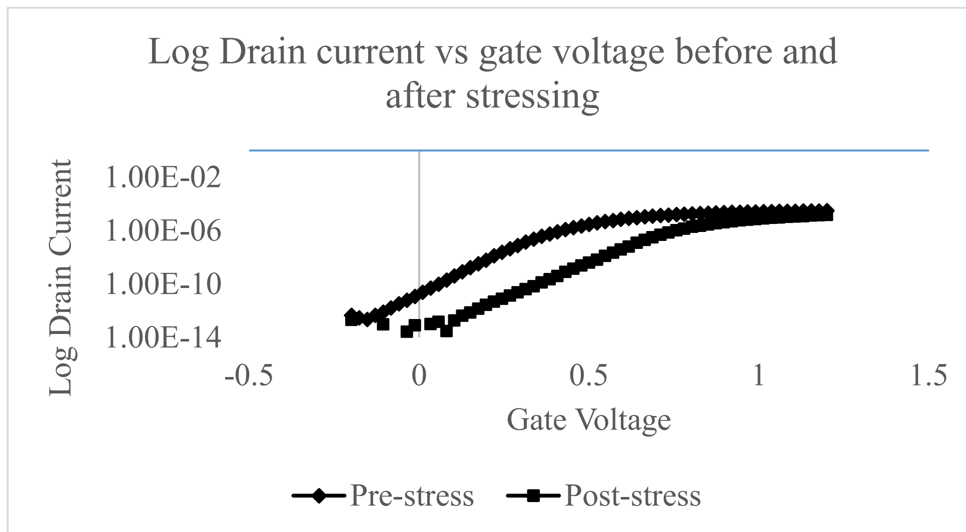

Figure 2.4 Plot Showing Increase in Subthreshold Swing Due to Hot Carrier Effect

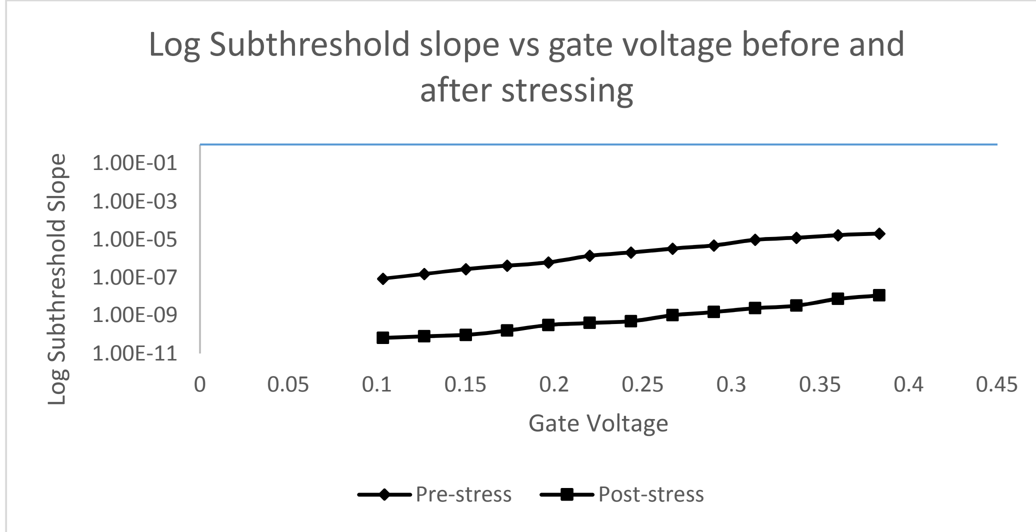

Figure 2.5 Plot Showing the decrease in Subthreshold Slope Due to Hot Carrier Effect

2.4.3 Hot Carrier Effect on the Mobility

Interface traps created during HCI degrades the mobility of the device by increasing coulomb scattering. An empirical relation between mobility and interface trap density is given as follows [49], [50],

$$\mu = \frac{\mu_0}{1 + \alpha N_{IT}}\,, \tag{2.3}$$

where, μ is the mobility after hot carrier degradation,

μ_0 is mobility of the device before degradation,

α is a constant that depends on doping concentration of the substrate and is given as,

$$\alpha = -0.104 + 0.0193\log(N_A)\,, \tag{2.4}$$

where, N_A is the doping concentration of the substrate.

2.4.4 Hot Carrier Effect on the Transconductance

The transconductance of a MOSFET is defined as the derivative of the drain current versus gate voltage. Therefore, transconductance is given as [39]:

$$g_m = \frac{\mu_n C_{OX} W}{L}(V_{GS} - V_{Th}) + \frac{1}{2} C_{OX}\left(\frac{W}{L}\right)(V_{GS} - V_{Th})^2 \left(\frac{\delta\mu_n}{\delta V_{GS}}\right), \qquad (2.5)$$

HCI decreases the mobility and increases the threshold voltage of a degraded devices, both these parameters lead to decrease in transconductance value as shown in the figure below [54].

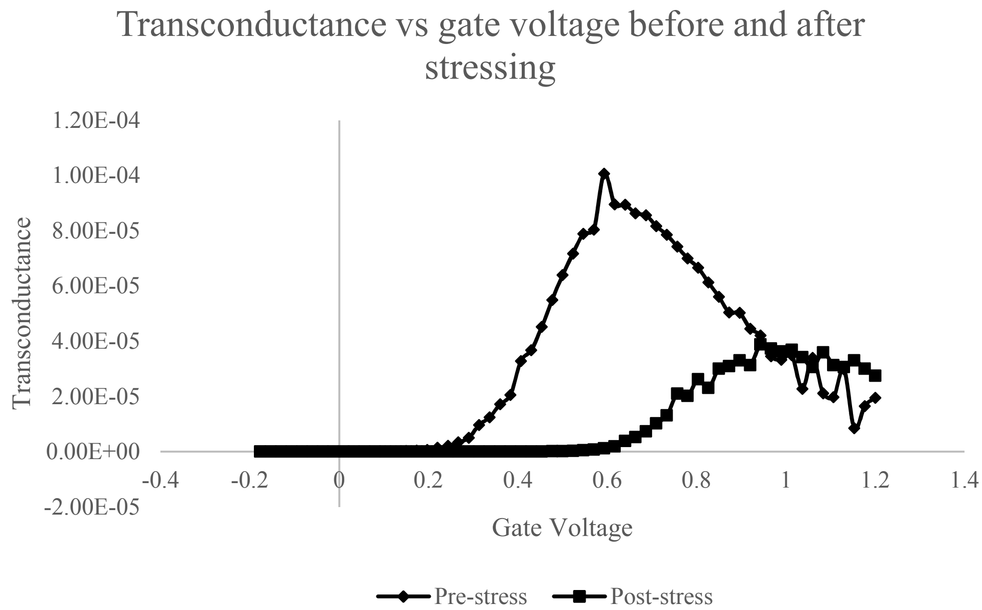

Figure 2.6 Plot Showing Decrease in Transconductance Due to Hot Carrier Effect

2.5 Hot Carrier Degradation in Long Channel MOSFET

The defects caused by HCI are localized in nature and extend for about 50nm - 200nm from the drain. Hence, in a long channel MOSFET conventional uniform defects

characterization techniques such as mid-gap techniques cannot be used [37], [51]. Whereas, in MOSFETs with channel length less than 50nm the defects are distributed all along the channel. Therefore in long channel MOSFET, because of non-uniform defect nature, the concept of single threshold voltage loses its meaning and two-piece transistor model is used to overcome this problem [51]. In this section, a detailed review of this defect localization, problems in characterizing because of it and a technique to overcome it is presented.

2.5.1 Location of Defects

When MOSFETs are biased in the saturation region of operation, the pinch off region appears near the drain terminal. Due to the existence of high field in the pinch off region, the carriers gain enough energy and undergo impact ionization generating electron-hole pairs which undergoes carrier injection. The carrier injection and defect generation are non-uniform along the channel because they depend on the local values of the carrier energy and vertical component of electric field [51].

Evidence for the localized nature of the defects is found in the asymmetrical behavior of the drain current characteristics, measured in the normal and reverse (source and drain interchanged) modes of operation. In the normal mode, as the drain bias increases the pinch off region expands towards the source and covers a larger portion of the defect region. As a result, the minority carriers flow far from the interface and are less affected due to the defects created. Therefore, the larger the drain bias the contribution due to damaged region is less and the drain current characteristics approaches that of non-degraded device. On the contrary, when the drain and source terminal are interchanged, the

reverse mode drain current is always less than that of non-degraded device because the damaged region of the channel falls inside the inversion region for all values of drain bias and so the defects are always active causing maximum degradation to drain current characteristics [14], [52]. This can be clearly seen in drain current versus drain bias plot shown in the figure below.

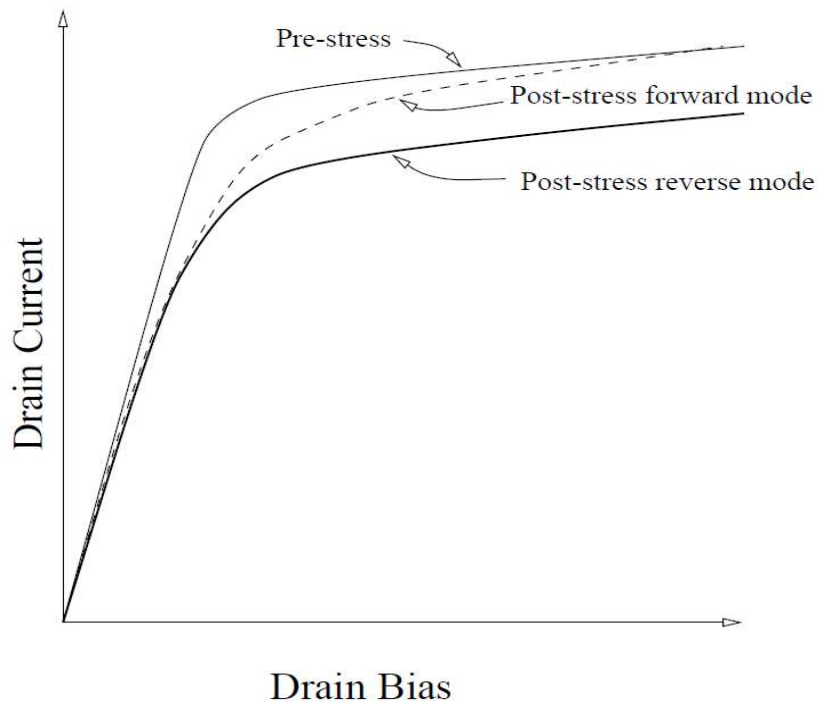

Figure 2.7 Normal and Reverse Mode Drain Current Vs Drain Bias Measured Before and After Hot Carrier Stress in NMOSFET [14]

The data above suggests that the defects generated due to HCI are localized near the pinch off region and it has been shown that the spreading of the defective region varies from 50nm to 200nm depending on the bias applied.

2.5.2 Problems Caused Due to Defect Localization in Measuring Degradation Parameters

During substrate hot carrier injection experiments, the carrier injection is uniform along the channel and the drain current characteristics can be used to provide details about the degradation processes [53], [54]. However, during drain avalanche hot carrier injection the carriers are injected into the gate-oxide in a localized region close to the drain and therefore, the interpretation of the parameter variations during non-uniform channel hot carrier injection based on the results obtained from uniform injection experiments can be highly inaccurate [51]. For example,

The change in drain current versus gate bias characteristics can be used to measure the density of interface traps and trapped charges in the gate oxide using the mid-gap voltage technique. This technique assumes that the change in subthreshold slope is entirely due to interface traps and the trapped charges cause only a parallel shift in the subthreshold characteristics of the drain current [37]. However, studies have shown that a localized oxide charge can also cause a change in subthreshold slope making the mid-gap technique useless.

When there is uniform injection of carriers, the threshold voltage at each point along the channel shifts by the same amount and therefore the threshold voltage of the complete device is equivalent to that of any point along the channel. However, during non-uniform injection of carriers, the threshold voltage at each point can be different due to localization of the defects. Hence, the definition of a single threshold voltage for an entire device loses it physical meaning [51].

2.5.3 Two-Piece Model

Most of the models which describe the hot carrier induced degradation do not account for defect localization and the defects are averaged over the entire channel length as if they were uniformly distributed [51].

Therefore, in order to have better understanding about the degraded parameter variation, the damaged transistor is considered as two transistors connected in series. One transistor with channel length equal to length of defective region with defects uniformly spread across the entire channel and the other transistor with no defects and channel length equal to length of non-defective region [55]. They are connected in series as shown in the figure.

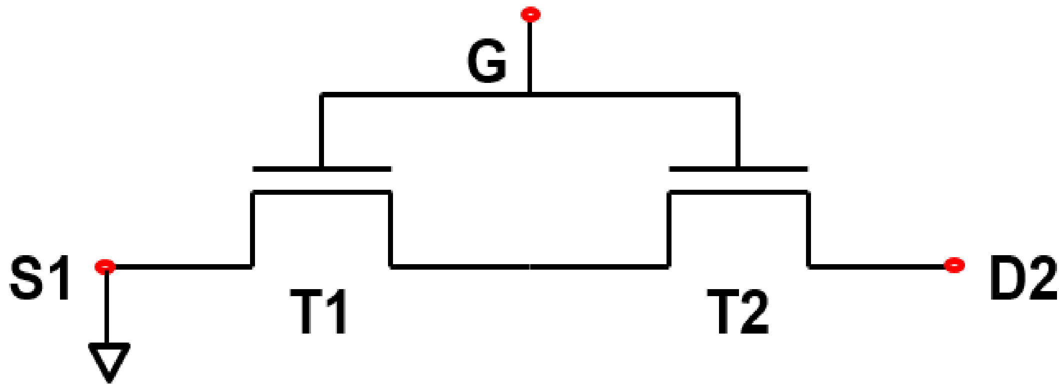

Figure 2.8 Schematic of Two Transistor Model

Let G1 and G2 be the conductance of the defect free and defective channel transistor and Ga and Gb are the conductance after and before HCI.

$$G_a = \frac{G_1 G_2}{G_1 + G_2}, \tag{2.6}$$

From the figure, it can be found that at the onset of strong inversion, the conductance G2 is very much lower than Gl and it is the defective region which dominates the current conduction through the channel. Whereas in the strong inversion, the defect free region regains the full control of the current conduction in the device.

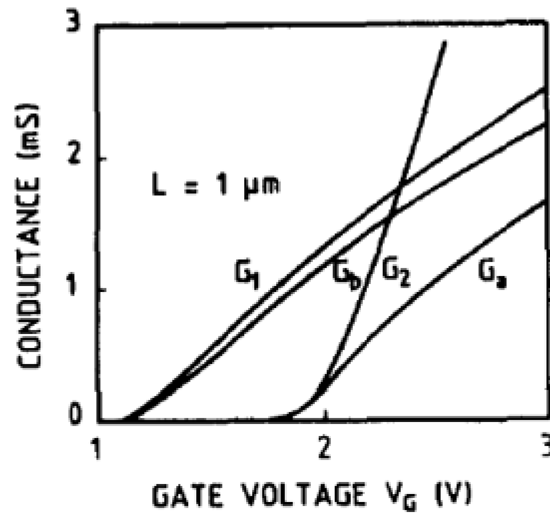

Figure 2.9 Channel Conductance Vs Gate Voltage [51]

Therefore, according to the two-piece model, the threshold voltage of a degraded device is the local threshold voltage value of the defective region. The damaged region exhibits a very low conductance when compared to the rest of the channel and no appreciable conduction takes place unless the gate bias exceeds the local threshold voltage of the defective region. On the other hand, one-piece model considers only one threshold value and it includes the average value of localized defects along the entire channel [51], [55].

3 HOT CARRIER INJECTION MODELS

3.1 Introduction

Theoretical work on hot carrier injection and its effects on the devices was started in early 1950s but the modelling was not started until 1980 [56]. This is mainly because, there is still debate going on about the different mechanisms involved in hot carrier injection such as, what charges get injected and whether charge injection is required to cause device degradation [11], [43].

However, experimental techniques have showed that hot carrier degradation is due to charge trapping and generation of interface traps and thus by measuring the device degradation parameters some models have been formulated [43], [57]. The lucky hot electron model proposed by Shockley is the widely-used model in studying the hot electron injection and using this, the gate current of the transistors was calculated theoretically [27], [13], [58]. Initially, the gate current was used to model the hot carrier effects but experiments have failed to show a good correlation between the gate current and defects created [11], [59], [60].

However, substrate current of MOSFETs have shown higher correlation to device degradation and by incorporating lucky electron model in substrate current calculation, relation between interface traps generated and substrate current was formulated [11], [60]. The problem with the above technique is that it considers only interface trap generation and not trapped charges in device degradation [11]. In this chapter, the concept of lucky

electron model is initially described and then the substrate current calculation based lucky electron model is presented.

3.2 Lucky Electron Model

The lucky electron model formulated by Shockley is one of the successful gate current models used in MOSFETs [61]. In this model, four statistically independent probabilities are calculated and the total probability corresponds to that of an electron travelling from the source to drain along the channel, being successfully able to overcome the potential barriers and get injected into the gate oxide and thus contributing to the gate current [27], [58], [61], [30], [62].

In order to quantify the probability that these electrons could be injected into the gate oxide, several types of scattering events have to be considered. Figure 3.1 shows an energy band diagram drawn normal to the Si-oxide interface along a cross section of the MOSFET in Figure 3.3.

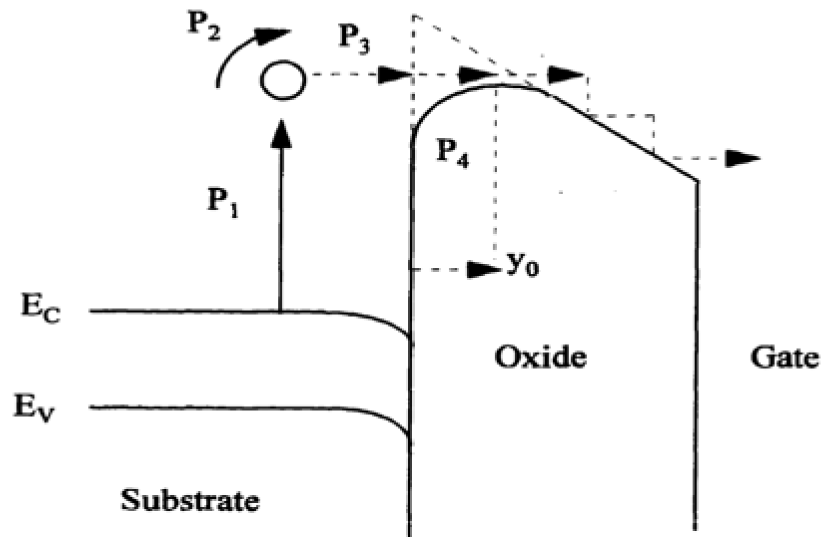

Figure 3.1 Schematic Showing Transverse Band Diagram in NMOSFET [62]

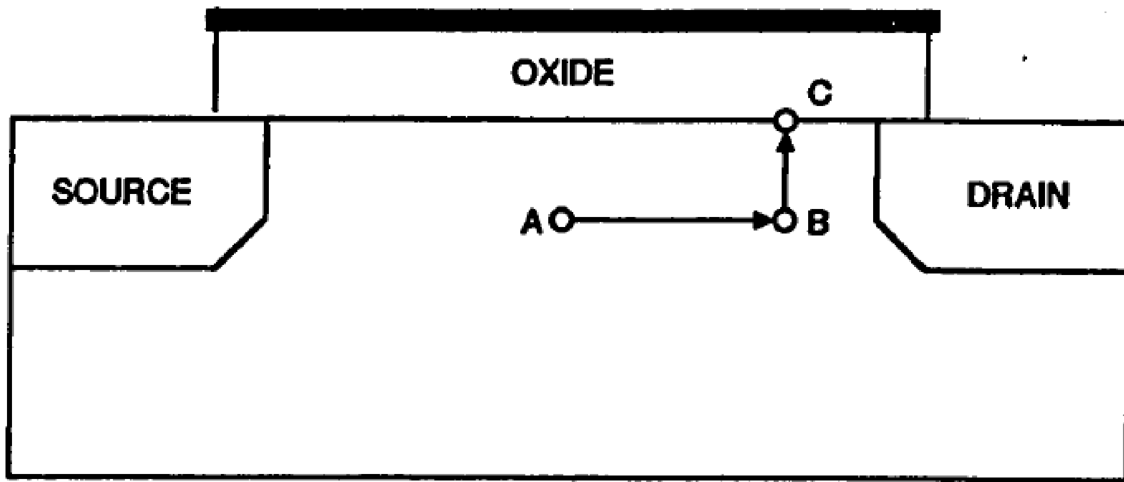

Figure 3.2 Scattering Events Associated With Lucky Hot Electron Model [63]

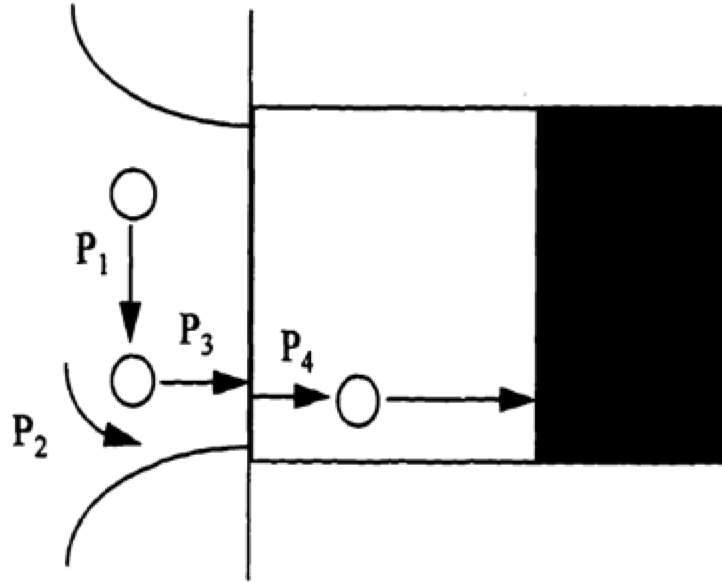

Figure 3.3 The Probabilities Associated With Lucky Hot Electron Model [62]

In Figure 3.2, an electron moving along the channel from point A to B, gains enough kinetic energy from the lateral electric field to cross the oxide-silicon interface potential barrier and this probability P1 is given by

$$P_1 = e^{-\frac{d}{\lambda}} = e^{-\frac{\phi_b}{E_x \lambda}}, \tag{3.1}$$

where, ϕ_b is the Schottky lowered barrier between silicon and gate oxide,

D is the distance an electron need to travel to acquire energy greater than ϕ_b,

Ex is the constant accelerating electric field between point A and B,

λ is the scattering mean free path of the hot electron in the silicon.

At point B, since the electron is travelling parallel to the interface, its momentum has to be redirected normal to the interface by an elastic collision. It should be noted that

this collision should not be an energy robbing collision, so that the electron will retain the kinetic energy required to surmount the oxide-silicon potential barrier and hence it is called quasi-elastic collision. Therefore, P2 gives the probability of this collision to take place and it is given by:

$$P_2 = \frac{1}{2}\left(1 - \sqrt{\frac{\phi_b}{\phi}}\right), \tag{3.2}$$

Thus, by integrating the product of P1 and P2 over all energies phi, the probability of an electron having enough normal momentum to surmount the oxide-silicon potential barrier can be calculated as,

$$P_1 P_2 = \frac{1}{4}\left(\frac{E_x \lambda}{\phi_b}\right) e^{-\frac{\phi_b}{E_g \lambda}}, \tag{3.3}$$

After the quasi-elastic collision, the electron must travel from point B to C at the interface without undergoing any further collisions so that its momentum does not get redirected or its kinetic energy does not get diminished. The probability P3 of this happening is given by,

$$P_3 = e^{-\frac{y}{\lambda}}, \tag{3.4}$$

where, y is the distance between point B and C.

Therefore, if the electron reaching the oxide interface has sufficient kinetic energy to overcome the oxide potential barrier, then it gets injected into the gate oxide. Since all the above three events are statistically independent, the carrier injection probability can be

obtained as the product of the probability of each event. However, the gate current consists only of electrons that overcome the image force potential well in the oxide and reach the gate electrode.

This probability P4 is given by

$$P_4 = e^{-\frac{y_0}{\lambda_{ox}}}, \qquad (3.5)$$

where, λ_{OX} is the scattering mean free path of the hot electrons in the oxide,

y_0 is the distance of the oxide potential maximum from the interface.

Therefore, the probability P, that an electron travelling in the channel reaches the gate terminal is given by the product of all this four probabilities. Thus, the number of electrons injected into the gate terminal per unit time per unit area is given as

$$J_{inj} = J_n(x, y)P, \qquad (3.6)$$

where, J_n is the electron current density in the channel.

Though the lucky electron model suffers from certain problems such as a large percentage of the electrons entering the gate oxide get scattered in the oxide and return to the silicon substrate, it remains one of the widely used model to calculate the injection current because of its simplicity.

3.3 Substrate Current Modelling

As technologies advance and MOSFET dimension decreases, the substrate current increases. This substrate current is used to characterize the degradation caused by hot

carrier injection because in both the device degradation and the substrate current the lateral electric field in the channel is the driving force [11], [60].

3.3.1 Origin of Substrate Current

When the MOSFET operates in the linear regime, the drain current increases linearly as the drain voltage increases. However, as the drain voltage is further increased, the channel thickness at the drain end gets reduced and at the voltage $V_D = V_{DSAT}$, the inversion layer gets pinched off. This corresponding voltage is called saturation drain voltage and if the drain voltage is increased beyond this point several important events occur: the length of the pinched off region increases and the voltage at the end of pinched off region remains sat Vdsat even if Vd increases. Therefore, the drain current remains almost constant but the electric field in the pinch off region increases rapidly. Due to this high electric field, electrons get accelerated and undergo several kinds of scattering events [62]. One such event is called impact ionization, where the electrons undergo collisions with the lattice and generates electron hole pairs. The holes created by this process are collected by the substrate and constitute the substrate current [11], [60]. Therefore, the substrate current can be given as

$$\mathrm{I_{sub}} = \mathrm{I_d r_{ii}}\ , \tag{3.7}$$

where, r_{ii} is the impact ionization rate which is dependent on the concentration of electrons in the channel and the lateral electric field.

Figure 3.4, is the plot of substrate current as a function of gate voltage for different drain voltages. Initially, when the gate voltage increases, the concentration of the electron

in the channel increases due to attraction by the gate voltage and hence substrate current increases. However, after a certain gate voltage, the lateral field in the channel decreases as shown in the Figure 3.5. This decrease in lateral electric field causes a decrease in substrate current. Thus, the change in equilibrium between the electron concentration and lateral electric field yields the bell shaped substrate current characteristics. The peak of the substrate current occurs at $V_G = V_D/2$ for older technology MOSFETs and at $V_G = V_D$ for latest technologies [11], [62].

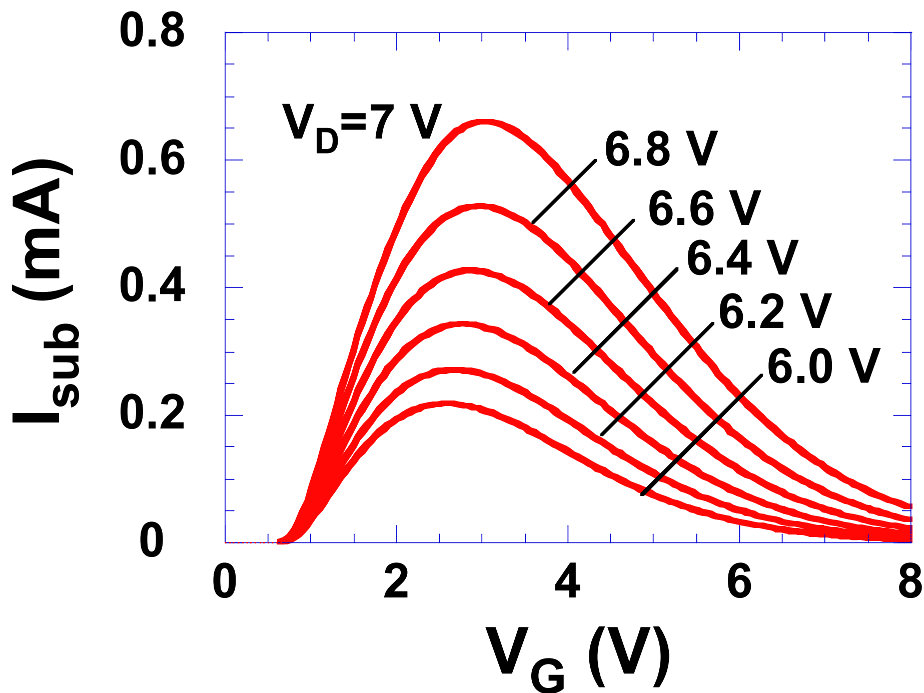

Figure 3.4 Plot Showing Substrate Current Vs Gate Bias for Different Drain Bias

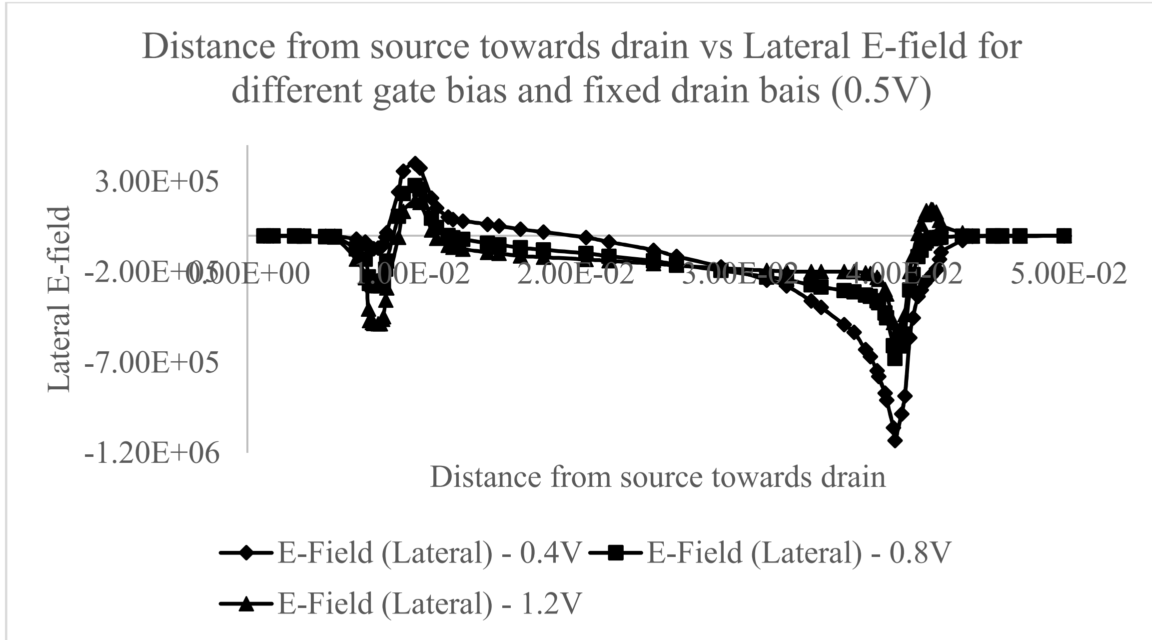

Figure 3.5 Plot Showing Decrease in Lateral Electric Field as Gate Bias Increased

3.3.2 Substrate Current Model Based on Lucky Electron Model

Using the lucky electron model approach, the impact ionization rate due to channel carriers can be calculated [64]. The electrons travelling along the channel must gain enough kinetic energy for generating electron-hole pairs through impact ionization process. The distance an electron needs to travel under the influence of the electric field in order to gain energy ϕ_i is given by

$$d = \frac{\phi_i}{qE_m}\ , \tag{3.8}$$

where, ϕ_i is the minimum energy required for by an electron to create impact ionization process.

E_m is the maximum electric field in the channel.

Thus the probability of an electron traveling a particular distance to be able to gain sufficient energy without undergoing a collision is given by

$$P_i = e^{-\frac{\phi_i}{q\lambda E_m}}, \qquad (3.9)$$

where, λ is the electron mean free path in the channel.

The drain current gives a measure of electron flow in the channel and the product of P_i*I_{ds} will give the rate at which electrons having energies greater than ϕ_i are supplied by the drain current. Therefore,

$$I_{sub} = CI_{ds}e^{-\frac{\phi_i}{q\lambda E_m}}, \qquad (3.10)$$

where, C is a function of E_m.

The interface traps created due to impact ionization can be calculated similarly. If the electron or hole have kinetic energy greater than what is required to break an oxide bond, then an interface trap will be created by them [64]. Let $\phi_{IT,E}$ and $\phi_{IT,H}$ be the energies required by the electrons and holes to create an interface trap and these values are found to be $\phi_{IT,E}$=3.7eV and $\phi_{IT,H}$=4.2eV which are determined experimentally.

Therefore, the portion of the drain current with electrons having kinetic energy greater than $\phi_{IT,E}$ can be given as

$$I_{BB,E} = \frac{C1}{W} I_{ds}e^{-\frac{\phi_{IT,E}}{q\lambda_e E_m}}, \qquad (3.10)$$

where, $I_{BB,E}$ is the bond breaking electron current.

λ_e is the mean free path of electrons in the channel.

Similarly, the portion of the substrate current with holes having kinetic energy greater than $\phi_{IT,H}$ can be given as

$$I_{BB,H} = \frac{C2}{W} I_{ds} e^{-\frac{\phi_{IT,H}}{q\lambda_h E_m}}, \tag{3.11}$$

where, $I_{BB,H}$ is the bond breaking hole current.

λ_h is the mean free path of holes.

The values of λ_e and λ_h are 6.7nm and 4.9nm respectively.

4 ANALYTICAL MODEL FOR HOT CARRIER DEGRADATION

4.1 Introduction

Most of the existing hot carrier degradation models do not consider the physics involved in the degradation process and they just calculate the change in threshold voltage for different stress voltages and time. Based on this threshold voltage shift, the lifetime of the device is predicted [65], [32], [11]. However, as seen from the previous chapters, hot carrier injection causes two types of traps namely, gate oxide trapped charges and interface traps and the effect of these traps on device parameters are different. Hence, the density of each type of traps created must be calculated individually.

In this chapter, a simple analytical model which calculates the density of trapped charges and interface traps is derived. In order to find out the parameters present in the analytical model, devices are stressed at different voltages and using the charge separation technique the density of trapped charges and interface traps are calculated. Once the parameters are determined, the validation of the analytical model is perform using TCAD simulations. Finally, the surface potential method is used to calculate the threshold voltage shift due to each type of traps and is incorporated in Verilog-A.

4.2 Derivation of Analytical Model

When an electron in the conduction band gain enough kinetic energy, then it might collide with the lattice and transfer its energy to the lattice causing it to break a bond and generate electron hole pairs. This process is called impact ionization as discussed in the previous section. These electron hole pairs generated by impact ionization can in turn gain

energy from the high electric field exiting in the pinch off region and further produce more electron hole pairs making it as a chain reaction. Such a chain reaction is called as avalanche impact ionization or avalanche multiplication and the electrons or holes generated by this method are called avalanche hot electrons or avalanche hot holes respectively [11], [62].

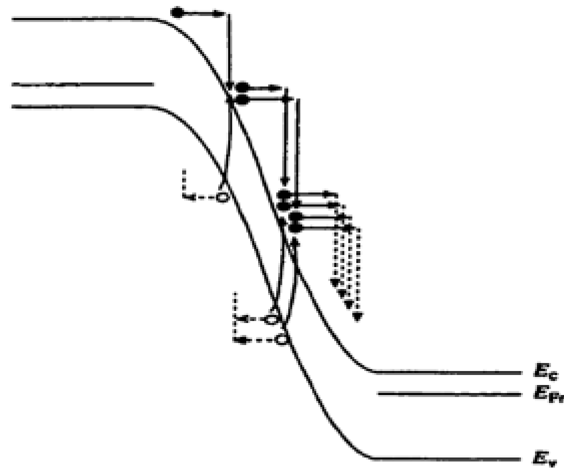

Figure 4.1 Carrier Multiplication Due to Impact Ionization [62]

At this point, when the drain voltage is increased, a sharp increase in the drain current is observed and this is called breakdown phenomenon and the drain voltage at which it occurs is called drain to source breakdown voltage. While the electrons generated reach either the drain electrode or the gate terminal, the holes move towards the substrate contributing to substrate current. This causes the potential of the substrate to increase above the source terminal and hence the potential barrier between the source and substrate gets lowered, which in turn further enhances electron injection and the drain current like a positive feedback loop [66].

Avalanche multiplication induced current can be given as

$$I_d = MI_s , \qquad (4.1)$$

where, I_d and I_s are the drain and source currents.

M is the multiplication factor and it can be given as

$$M = \frac{1}{1 - I_{ion}} , \qquad (4.2)$$

where, I_{ion} is the ionization integral which can be defined as

$$I_{ion} = \int \alpha_n e^{-\int^x (\alpha_n - \alpha_p)dx} \, dx', \qquad (4.3)$$

where, α_n and α_p are the ionization rates of electrons and holes respectively. In order to understand hot carrier degradation, it was realized that an accurate model calculating the electric field is required [67], [68]. By using the pseudo two dimensional approximation and Poisson's equation, an expression for electric field in the channel is derived as

$$E(x) = E_{sat} \cosh\left(\frac{x - x_{sat}}{l}\right), \qquad (4.4)$$

where, E_{sat} is the critical electric field needed for velocity saturation,

x is the distance from the source in the channel towards drain,

l is the effective length of the velocity saturation region,

x_{sat} is the point at which E equals Esat.

Using the above expression the maximum electric field in the channel is given as

$$E_m = \sqrt{A^2(V_{ds} - V_{dsat})^2 + E_{sat}^2}\,, \qquad (4.5)$$

Thus the substrate current can be expressed as,

$$I_{sub} = \frac{\alpha_i}{\beta_i} I_{ds}(V_{ds} - V_{dsat}) e^{-\frac{A}{V_d - V_{dsat}}}\,, \qquad (4.6)$$

where, α_i and β_i are impact ionization coefficients and A is a fitting parameter [62], [69], [70]. Substrate current gives a quantitative measurement of the number of holes, and therefore electrons, generated through impact ionization.

A simple model to estimate the density of trapped charges and interface traps generated is formulated using the above model. If the device is stressed for t seconds and I_{sub} is the substrate current, then the total amount of charges generated can be given as,

$$Q = I_{sub} t\,, \qquad (4.7)$$

Some percentage of these charges will contribute to generation of interface traps and some will get trapped in the gate oxide. Therefore, the density of trapped charges and interface traps generated can be given as,

$$N_{ot} = k_{not} Q\,, \qquad (4.8)$$

$$N_{it} = k_{nit} Q\,, \qquad (4.9)$$

where, K_{not} and k_{nit} are the fitting parameters which are determined using the experimental data.

Since the substrate current depends on gate and drain voltages, the analytical formula used here to calculate the device degradation is a function of these stress voltages and stress time.

4.3 Model Parameterization and Validation

As presented above, the analytical model used in this thesis is based on the substrate current and the amount of charges created by them.

$$I_{sub} = \frac{\alpha_i}{\beta_i} I_{ds}(V_{ds} - V_{dsat}) e^{-\frac{A}{V_d - V_{dsat}}}, \tag{4.10}$$

where, α_i and β_i are impact ionization coefficients and A is the parameter which is dependent on the applied stress voltage.

From the substrate current, the density of trapped charges and interface traps generated can be given as,

$$N_{ot} = k_{not} I_{sub} t, \tag{4.11}$$

$$N_{it} = k_{nit} I_{sub} t, \tag{4.12}$$

where, t is the amount of time the device is stressed for a given stress voltage and k_{not} and k_{nit} are the fitting parameters. Therefore, the parameters which need to be calculated using the experimental data are k_{not}, k_{nit} and A, in which k_{not} and k_{nit} are constant for all stress voltages and A depends on the applied stress voltage.

Following the model parametrization, using the analytical model, the density of trapped charges and interface traps generated are calculated for different stress voltages

and compared against the results of TCAD simulations to verify the accuracy of the model and the parameters obtained.

In the next section, a method used to separate the density of oxide trapped charges and interface traps generated from the drain current characteristics is presented and the traps generated are calculated from the data for different stress voltage. Finally, the various parameters are calculated and is validated against TCAD simulations.

4.3.1 Charge Separation Technique

As seen from previous chapters, hot carrier injection in MOSFET causes interface trap generation and charge trapping in gate oxide, thereby causing change in sub-threshold slope and threshold voltage of the device. The total threshold shift due to these two defects can be given as [37], [71],

$$\delta V_{Th} = \delta V_{not} + \delta V_{nit}\,, \tag{4.13}$$

where δV_{not} is threshold shift due to oxide trapped charges and

δV_{dit} is the threshold shift due to interface traps.

Two techniques are available to calculate the trapped charge density and interface trap density from the device characteristics [71], [72]. The inversion characteristics technique uses Brews charge sheet model to fit the experimental data and it requires an empirical coefficient, actual physical dimensions of the transistors and other process parameters which are not easily available [72], [73]. The other technique namely, mid-gap voltage method requires only the gate oxide thickness and the substrate doping which are easier to extract using the data and TCAD simulations and also in the case of short channel

MOSFETs, the defects are spread across the entire channel length. Hence the mid-gap voltage method can be employed.

The assumptions made in this method are [37]:

1. The negative fixed trapped charge (electron) density is a sheet of charge at the interface which is spread across the entire channel length and

2. Acceptor like interface traps are present only in the upper half of the bandgap and donor like interface traps are present only in the lower half of the bandgap. Therefore, when the surface potential is equal to the bulk potential that is when the Fermi level touches the intrinsic level at the interface, the net charge contribution by the interface states are zero and this corresponding voltage is called mid-gap voltage.

In NMOS, the interface traps generated decrease the subthreshold slope and increase the threshold voltage whereas, the trapped electrons cause only increase in threshold voltage. Since at the mid-gap voltage the interface traps are neutral, the change in drain current characteristics in the Id-Vgs plot is only due to charges trapped in the oxide [37], [71]. Thus the shift in the mid-gap voltage level (δV_{mg}) is equal to voltage shift due to trapped electrons (δV_{not}), that is,

$$\delta \mathrm{V_{mg}} = \delta \mathrm{V_{not}}\,, \tag{4.14}$$

and the threshold shift due to interface states can be calculated from the total threshold voltage shift by,

$$\delta \mathrm{V_{nit}} = \delta \mathrm{V_{Th}} - \delta \mathrm{V_{not}}\,, \tag{4.15}$$

The drain current in the subthreshold region is given by [5]:

$$I_d = \mu\left(\frac{W}{L}\right)\left(\frac{aC_{OX}}{2\beta^2}\right)\left(\frac{n_i}{N_A}\right)^2\left(1 - e^{-\beta V_d}\right)\left(\frac{e^{\beta\phi_s}}{\sqrt{\beta\phi_s}}\right), \quad (4.16)$$

where

$$a = \frac{\sqrt{2}\epsilon_s}{C_{OX}L_D}, \quad (4.17)$$

$$L_D = \sqrt{\frac{\epsilon_s}{\beta q N_A}}, \quad (4.18)$$

And where μ is the mobility of the electron in the channel,

L_D is the Debye length,

W is the width of the transistor,

L is the channel length,

Cox is the gate oxide capacitance,

N_A is the doping concertation of the substrate,

n_i is intrinsic,

ϕ_s is the surface potential;

The mid-gap current can be calculated from the above equation by using,

$$\phi_s = \phi_b = \frac{kT}{q}\ln\left(\frac{N_A}{n_i}\right), \quad (4.19)$$

where, ϕ_b is the bulk potential.

Therefore,

$$I_{mg} = \mu\left(\frac{W}{L}\right)\left(\frac{aC_{OX}}{2\beta^2}\right)\left(\frac{n_i}{N_A}\right)^2\left(1 - e^{-\beta V_d}\right)\left(\frac{e^{\beta\phi_b}}{\sqrt{\beta\phi_b}}\right), \quad (4.20)$$

The mid-gap voltage is the gate voltage at which drain current equals I_{mg} and since this current is less than that of leakage current, the drain current must be extrapolated to determine the mid-gap voltage [71].

Threshold voltage is the voltage at which surface potential is twice that of the bulk potential. So the drain current at the threshold voltage can be found by using,

$$\phi_s = 2\phi_b = 2\frac{kT}{q}\ln\left(\frac{N_A}{n_i}\right), \quad (4.21)$$

Therefore,

$$I_{Vt} = \mu\left(\frac{W}{L}\right)\left(\frac{aC_{OX}}{2\beta^2}\right)\left(\frac{n_i}{N_A}\right)^2\left(1 - e^{-\beta V_d}\right)\left(\frac{e^{2\beta\phi_b}}{\sqrt{2\beta\phi_b}}\right), \quad (4.22)$$

The voltage that corresponds to this current in the drain current vs gate voltage characteristics gives us the threshold voltage.

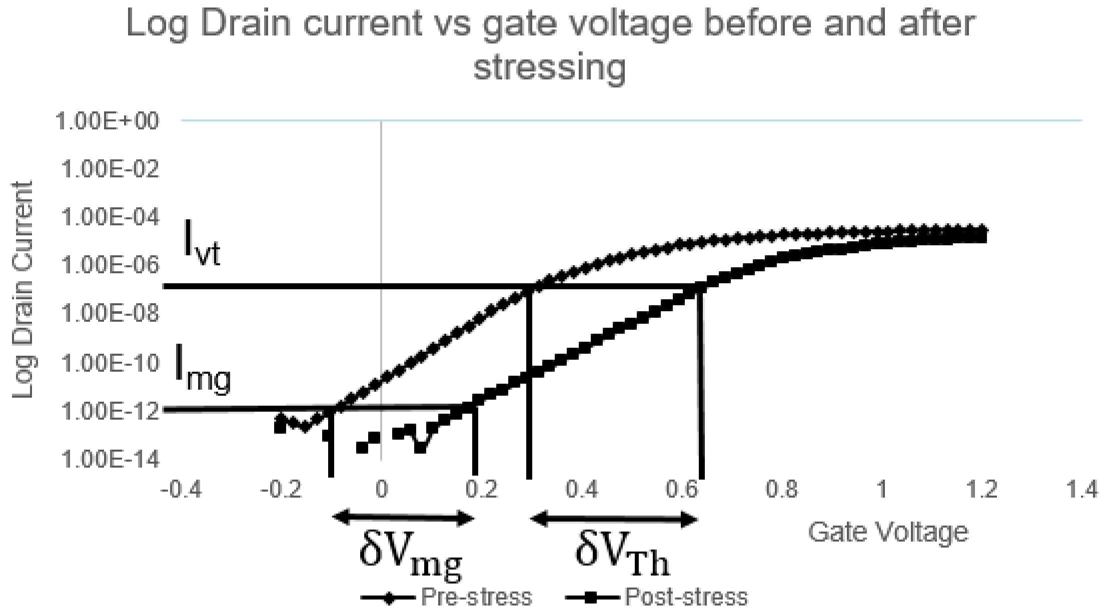

Figure 4.2 Plot Showing Log Drain Current Vs Gate Voltage and Mid-gap Current and Threshold Voltage Current

4.3.2 Extraction of Fixed Charge and Interface Trap Density from the Data

In order to find out the values of different parameters, five different devices are stressed at different voltages. The value of gate oxide thickness and substrate doping is calculated by matching the pre-stressed data of each device with TCAD simulations. Plots showing the pre-stress data and TCAD simulations are shown below. The difference in drain current characteristics at higher gate voltage is because of the different mobility models available in TCAD.

A small difference between each device's oxide thickness and doping concentration was observed which is due to process variability. The table attached below shows each device gate oxide thickness, their doping concentration and the applied stress voltage.

	Stress Voltage (V) Gate Voltage = Drain Voltage	Doping Concentration (cm^{-3})	Gate Oxide Thickness (cm)
Device 1	1.2	6.8E18	1.1E-7
Device 2	1.4	5.3E18	1.3E-7
Device 3	1.6	5.9E18	1.3E-7
Device 4	1.8	5.9E18	1.2E-7
Device 5	2	6.1E18	1.1E-7

Table 4.1 Each Device's Doping Concentration, Oxide Thickness and the Voltage at Which They Are Stressed

Since the oxide thickness and substrate doping are known, the mid-gap current and the threshold current for each device can be calculated using the subthreshold drain current equation which is given by [89],

$$I_d = \mu\left(\frac{W}{L}\right)\left(\frac{aC_{OX}}{2\beta^2}\right)\left(\frac{n_i}{N_A}\right)^2\left(1 - e^{-\beta V_d}\right)\left(\frac{e^{\beta\phi_s}}{\sqrt{\beta\phi_s}}\right), \quad (4.23)$$

From the above equation, the mid-gap current can be calculated by substituting,

$$\phi_s = \phi_b = \frac{kT}{q}\ln\left(\frac{N_A}{n_i}\right), \quad (4.24)$$

Similarly, the threshold current can be found by substituting,

$$\phi_s = 2\phi_b = 2\frac{kT}{q}\ln\left(\frac{N_A}{n_i}\right), \quad (4.25)$$

The I_{mg} and I_{vth} for each device is listed in the below table. The mid-gap voltage method is used to extract the oxide trapped charge density and interface trap density as seen from the above section [37], [71].

Both the pre-stressed and post-stressed drain currents are extrapolated in the log Id vs gate voltage plot as shown in the Figure 4.2. The voltage corresponding to mid-gap current and threshold current is found for both the pre-stressed and post-stressed condition in all the five devices.

	Mid-gap Current (A) I_{Mg}	Threshold Current (A) I_{Th}	Mid-gap Voltage (V) V_{Mg}		Threshold Voltage (V) V_{Th}	
			Pre-stress	Post-stress	Pre-stress	Post-stress
Device 1	6.68E-16	3.21E-7	-0.30472	-0.30278	0.367682	0.369993
Device 2	7.61E-16	2.85E-7	-0.37705	-0.37375	0.313298	0.319828
Device 3	7.19E-16	3.01E-7	-0.32832	-0.27975	0.349384	0.413454
Device 4	7.19E-16	3.01E-7	-0.34368	-0.24123	0.330669	0.475805
Device 5	7.07E-16	3.05E-7	-0.33847	-0.12845	0.320869	0.667041

Table 4.2 Mid-gap Current and Threshold Voltage Current for Different Device and the Corresponding Mid-gap Voltage and Threshold Voltage for Pre-stress and Post-stress Condition

The change in mid-gap voltage between pre-stressed and post-stressed condition gives the change in voltage due to trapped charges since interface traps are neutral at this condition.

Therefore,

$$\delta V_{mg} = \delta V_{not} , \tag{4.26}$$

The threshold shift due to interface traps alone can be given by;

$$\delta V_{nit} = \delta V_{Th} - \delta V_{not} , \tag{4.27}$$

The table attached gives δV_{Th}, δV_{not} and δV_{nit} for each of device. From δV_{not} and δV_{nit}, the density of trapped charges and interface traps can be calculated by;

$$N_{it} = \frac{C_{OX}\delta V_{nit}}{q} , \quad (4.28)$$

$$N_{ot} = \frac{C_{OX}\delta V_{not}}{q} , \quad (4.29)$$

where, C_{ox} is the gate oxide capacitance. The density of trapped charges and interface traps generated for different stress voltages calculated from the data using mid-gap method are listed in the below table. TCAD simulations are done using the values obtained from the mid-gap voltage technique and the drain current characteristics is shown in the figure below. The difference in strong inversion region drain currents are due to mobility models in TCAD.

Stress Voltage (V)	$\Delta V_{Mg} = \Delta V_{NOT}$ (V)	ΔV_{Th} (V)	$\Delta V_{NIT} = \Delta V_{Th} - \Delta V_{NOT}$ (V)	NOT = $Cox*\Delta V_{Mg}/q$ (cm^{-2})	NIT = $Cox*\Delta V_{NIT}/q$ (cm^{-2})
1.2	0.00194	0.002311	0.000371	3.7E10	7.5E9
1.4	0.0033	0.00653	0.00323	5.5E10	5.3E10
1.6	0.04857	0.06407	0.0155	8E11	2.6E11
1.8	0.10245	0.145136	0.042686	1.8E12	7.6E11
2	0.21002	0.346172	0.136152	4.1E12	2.6E12

Table 4.3 Density of Trapped Oxide Charges and Interface Traps Generated for Different Stress Voltage

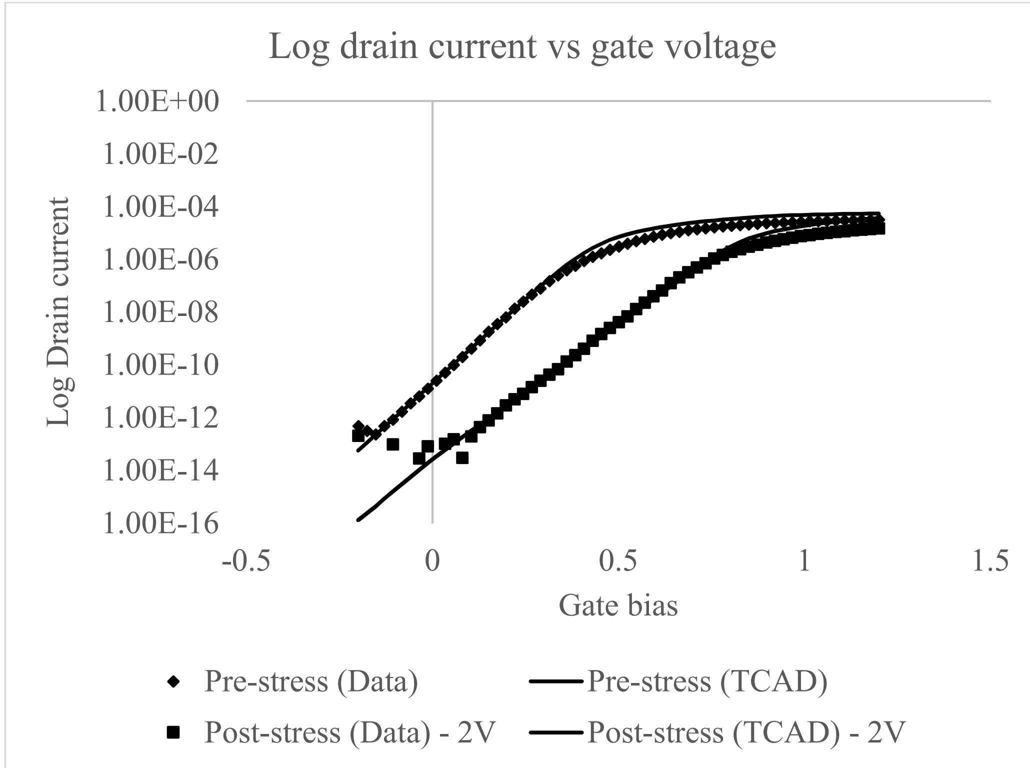

Figure 4.3 Plot Showing Pre-stress and Post-stress of Both Data and TCAD Simulation With Density of Traps Value Obtained Using Mid-gap Voltage Method

4.3.3 TCAD Validation

From the substrate current equation, the parameter A can be expressed as,

$$A = x\ln(cx) \tag{4.30}$$

where, c is a constant and

x is a function of applied stress voltage and drain current.

The above expression can be expanded using the Taylor series and thus and thus the parameter A can be written as a function of stress voltage in the quadratic form.

In order to get an approximate value of the parameter A, the substrate current and the drain current are measured for different stress voltages. Having known the substrate

current, the density of oxide trapped charges and interface traps, the parameters k_{not} and k_{nit} can be calculated as follows,

$$k_{not} = \frac{N_{ot}}{qI_{sub}}\ , \tag{4.31}$$

$$k_{nit} = \frac{N_{it}}{qI_{sub}}\ , \tag{4.32}$$

The validation of the analytical model is done using TCAD simulations and the data. From the analytical model, the density of trapped charges and interface traps generated are calculated for different stress voltages and the table below shows these values. Using these trap values in TCAD, the drain current characteristics are calculated for different stress voltages and is compared against the data. The plots are shown below.

Stress Voltage (V)	NOT (cm^{-2})		NIT (cm^{-2})	
	Analytical model	From Data	Analytical model	From Data
1.2	3E10	3.7E10	1.6E10	7.5E9
1.4	6.6E10	5.5E10	3.7E10	5.3E10
1.6	5.1E11	8E11	2.8E11	2.6E11
1.8	1.5E12	1.8E12	8.2E11	7.7E11
2	4.2E12	4.1E12	2.3E12	2.6E12

Table 4.4 Density of Traps Calculated Using Analytical Model and from the Data

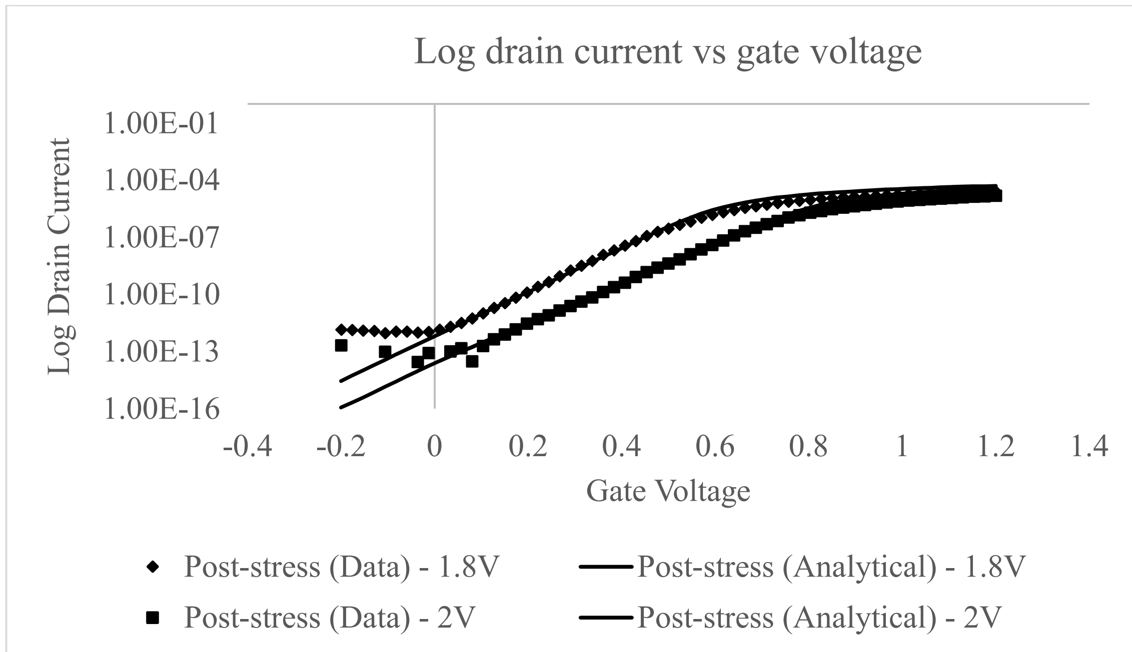

Figure 4.4 Plots Comparing Post-stress Condition Between Analytical Method and Data

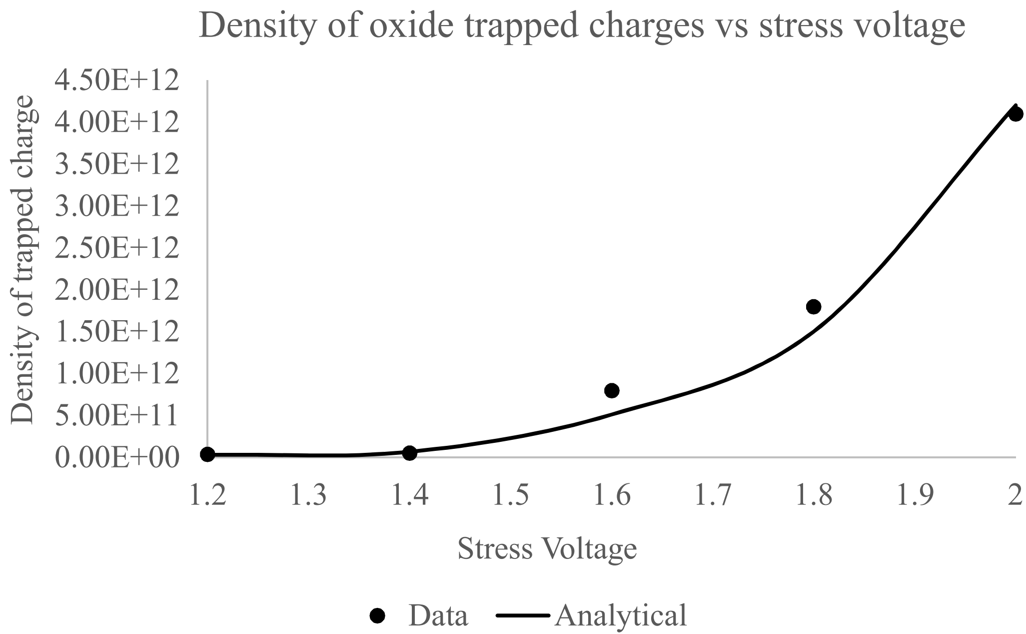

Figure 4.5 Plot Comparing N_{ot} Calculated Using Analytical Model and Using Data

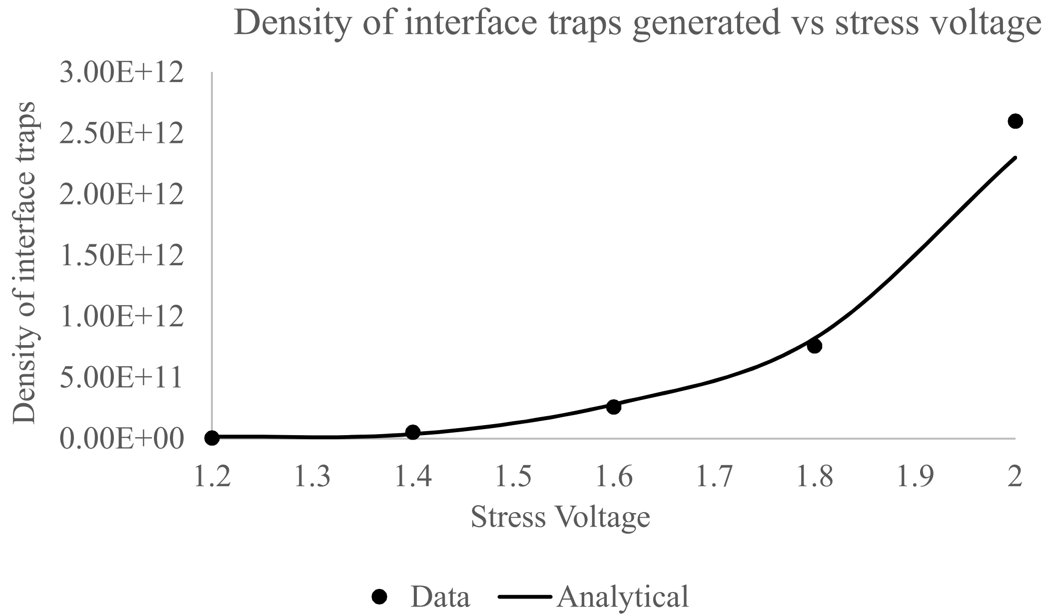

Figure 4.6 Plot Comparing N_{it} Calculated Using Analytical Model and Using Data

4.4 Incorporating the Analytical Model Using Surface Potential Method

Using the analytical expression, the density of oxide trapped charges and interface traps generated are calculated. However, in order to use them in circuits, the effect of these traps on device parameters have to be calculated using a surface potential method and must be incorporated using Verilog-A [74], [75]. In this method, the effect of oxide trapped charges and interface traps on surface potential are modelled and using the surface potential – gate voltage relationship, the total impact on the device is calculated.

According to Gauss theorem, the amount of charge per unit area is given as,

$$Q_s = -\epsilon_s E_s = -\mathrm{sgn}(\phi_s) Q_0 \sqrt{H(\beta\phi_s)}\,, \tag{4.33}$$

$$Q_0 = \sqrt{2q\epsilon_s \phi_t N_A}\,, \tag{4.34}$$

where, ϵ_s is the semiconductor permittivity and

E_s is the surface electric field,

ϕ_t is the thermal voltage,

Na is the doping concentration,

The function $H(\beta\phi_s)$ can be written as [74],

$$H(\beta\phi_s) = (e^{-\beta\phi_s} + \beta\phi_s - 1) + e^{-\beta(2\phi_b+\phi_n)}(e^{\beta\phi_s} - \beta\phi_s - 1), \quad (3.35)$$

where, ϕ_n is the split in quasi Fermi level.

The gate voltage can be expressed in terms of surface potential as,

$$V_g = V_{fb} + \phi_s + \frac{\sqrt{2q\epsilon_s N_A}}{C_{OX}} \mathrm{sgn}(\phi_s)\sqrt{\phi_s H(\beta\phi_s)}\,, \quad (4.36)$$

where, V_{fb} is the flatband voltage and it is a function of interface traps generated and trapped oxide charges, that is,

$$V_{fb} = \phi_{MS} - \frac{Q_{it}(\phi_s)}{C_{OX}} - \frac{Q_{not}}{C_{OX}}\,, \quad (4.37)$$

where, ϕ_{MS} is the work function difference between the gate metal and semiconductor.

The effect of traps can be incorporated into gate voltage and surface potential equation by defining a new term called defect potential parameter ϕ_{nt} and therefore,

$$V_g = \phi_{MS} - \phi_{nt} + \phi_s + \frac{\sqrt{2q\epsilon_s N_A}}{C_{OX}} \mathrm{sgn}(\phi_s)\sqrt{\phi_s H(\beta\phi_s)}\,, \quad (4.38)$$

where,

$$\phi_{nt} = \frac{q}{C_{OX}}\left(N_{ot} - D_{it}(\phi_s - \phi_b)\right), \tag{4.39}$$

Using the analytical model, the density of traps created are calculated and based on which the defect potential is found out and correspondingly the effective gate voltage. Finally, this is incorporated in circuits using Verilog-A.

5 CONCLUSION

In this thesis, various hot carrier injection mechanisms and the reason for more degradation in NMOSFET was discussed. Hot carrier injection causes degradation in devices due to carrier injection in gate oxide and due to generation of interface traps. The effect of these traps are different, while trapped charges contribution to device parameters are independent of applied gate bias, the effect of interface traps depend on gate bias. For instance, only interface traps cause change in the subthreshold slope of drain current characteristics whereas, trapped charges do not cause any change to subthreshold slope if it is non-localized. Because of these traps various parameters such as subthreshold slope, threshold voltage, mobility and transconductance of the device gets affected.

The traps are localized near the drain region and the range extends from 50nm- 100nm depending on the stress time. Therefore, in long channel MOSFETs a general method used to calculate density of traps cannot be used and the concept of single threshold voltage loses its meaning. Hence, a simple two piece model is used. In case of short channel MOSFETs, mid-gap voltage method can be used to extract the density of trapped charges and interface traps separately from the data.

The lucky hot electron gate current model and substrate current model are the two most widely accepted hot carrier injection models and they were presented. Most of the hot carrier degradation models are based on calculating the shift in threshold voltage and thereby predicting the lifetime of the device. The problem with these models are, they

ignore the effect of traps individually, therefore a degradation model considering their effect separately will be more relevant.

In this thesis, an analytical model calculating the density of trapped charges in gate oxide and interface traps generated is formulated and it is a function of stress voltage and time. This model is parametrized using the data obtained by stressing the device at different stress voltages. TCAD simulations are used to validate the analytical model and it showed very good match. Finally, this analytical model is incorporated in the circuits using surface potential method using Verilog-A. In this method, a defect potential parameter is calculated using the density of traps value obtained from the analytical expression.

REFERENCES

[1] G. E. Moore, “Cramming More Components Onto Integrated Circuits,” *Proc. IEEE*, vol. 86, no. 1, pp. 82–85, Jan. 1998.

[2] ITRS, “International technology roadmap for semiconductors 2013; Executive Summary,” *Itrs*, 2013.

[3] A. Reisman, “Device, circuit, and technology scaling to micron and submicron dimensions,” *Proc. IEEE*, vol. 71, no. 5, pp. 550–565, 1983.

[4] C. T. Wang, Ed., *Hot Carrier Design Considerations for MOS Devices and Circuits*. Boston, MA: Springer US, 1992.

[5] S. M. Sze and K. K. Ng, “Physics of Semiconductor Devices, 3rd Edition - Simon M. Sze, Kwok K. Ng,” *Phys. Semicond. Devices, 3rd Ed. John Wiley Sons, Inc.; NJ*, 2007.

[6] K. O. Jeppson and C. M. Svensson, “Negative bias stress of MOS devices at high electric fields and degradation of MNOS devices,” *IEEE J. Appl. Phys.*, 1977.

[7] Y. Kiinizuka *et al.*, “The impact of bias temperature instability for direct-tunneling ultra-thin gate oxide on MOSFET scaling,” *Syrnposlurn VLSl Technol.*, 1999.

[8] “http://www.siliconfareast.com/oxidebreakdwon.html.” .

[9] “http://www.siliconfareast.com/hotcarriers.html.” .

[10] T. H. Ning, P. W. Cook, R. H. Dennard, C. M. Osburn, S. E. Schuster, and H. Yu, “1 µm MOSFET VLSI technology: Part IV—Hot-electron design constraints,” *IEEE Trans. Electron Devices*, vol. 26, no. 4, pp. 346–353, Apr. 1979.

[11] Chenming Hu, Simon C. Tam, Fu-Chieh Hsu, Ping-Keung Ko, Tung-Yi Chan, and K. W. Terrill, “Hot-Electron-Induced MOSFET Degradation - Model, Monitor, and Improvement,” *IEEE J. Solid-State Circuits*, 1985.

[12] V. H. Chan and J. E. Chung, “The Impact of NMOSFET Hot-Carrier Degradation on CMOS Analog Subcircuit Performance,” *IEEE J. Solid-State Circuits*, 1995.

[13] C. Hu, “Lucky-electron model of channel hot electron emission,” *Iedm*, 1979.

[14] M. P. Pagey, “CHARACTERIZATION AND MODELING OF HOT-CARRIER DEGRADATION IN SUB-MICRON NMOSFETS,” Vanderbilt University, 2002.

[15] Y. Nissan-Cohen, J. Shappir, and D. Frohman-Bentchkowsky, “Trap generation and occupation dynamics in SiO2 under charge injection stress,” *J. Appl. Phys.*, 1986.

[16] B. Doyle, M. Bourcerie, J.-C. Marchetaux, and A. Boudou, “Interface state creation and charge trapping in the medium-to-high gate voltage range during hot-

carrier stressing of n-MOS transistors," *IEEE Trans. Electron Devices*, vol. 37, no. 3, pp. 744–754, Mar. 1990.

[17] S. J. Wang, J. M. Sung, and S. A. Lyon, "Relationship between hole trapping and interface state generation in metal□oxide□silicon structures," *Appl. Phys. Lett.*, vol. 52, no. 17, pp. 1431–1433, Apr. 1988.

[18] S. K. Lai, "Two-carrier nature of interface-state generation in hole trapping and radiation damage," *Appl. Phys. Lett.*, 1981.

[19] Y. Roh, L. Trombetta, and D. J. DiMaria, "Interface traps induced by hole trapping in metal-oxide semiconductor devices," *J. Non. Cryst. Solids*, vol. 187, pp. 165–169, Jul. 1995.

[20] Y. Leblebici and S.-M. Kang, *Hot-Carrier Reliability of MOS VLSI Circuits*. Boston, MA: Springer US, 1993.

[21] H. Hara, Y. Okamoto, and H. Ohnuma, "A New Instability in MOS Transistor Caused by Hot Electron and Hole Injection from Drain Avalanche Plasma into Gate Oxide," *Jpn. J. Appl. Phys.*, vol. 9, no. 9, pp. 1103–1112, Sep. 1970.

[22] S. A. Abbas and R. C. Dockerty, "Hot□carrier instability in IGFET's," *Appl. Phys. Lett.*, vol. 27, no. 3, pp. 147–148, Aug. 1975.

[23] T. H. Ning, C. M. Osburn, and H. N. Yu, "Effect of electron trapping on IGFET characteristics," *J. Electron. Mater.*, vol. 6, no. 2, pp. 65–76, Mar. 1977.

[24] J. MA and C. Science, "STUDY OF GATE OXIDE BREAKDOWN AND HOT ELECTRON EFFECT ON CMOS CIRCUIT PERFORMANCES," University of Central Florida, 2009.

[25] S. NASEH, "INVESTIGATION OF HOT CARRIER EFFECTS ON RF CMOS INTEGRATED CIRCUITS," McMaster University, 2005.

[26] T. Poorter and P. Zoestbergen, "Hot carrier effects in MOS transistors," in *1984 International Electron Devices Meeting*, 1984, pp. 100–103.

[27] T. H. Ning, C. M. Osburn, and H. N. Yu, "Emission probability of hot electrons from silicon into silicon dioxide," *J. Appl. Phys.*, vol. 48, no. 1, pp. 286–293, Jan. 1977.

[28] K. N. Quader, E. R. Minami, Wei-Jen Ko, P. K. Ko, and Chenming Hu, "Hot-carrier-reliability design guidelines for CMOS logic circuits," *IEEE J. Solid-State Circuits*, vol. 29, no. 3, pp. 253–262, Mar. 1994.

[29] E. Takeda, "A cross section of VLSI reliability-hot carriers, dielectrics and metallization," *Semicond. Sci. Technol.*, vol. 9, no. 5, pp. 971–987, May 1994.

[30] K. R. Hofmann, C. Werner, W. Weber, and G. Dorda, "Hot-electron and hole-emission effects in short n-channel MOSFET's," *IEEE Trans. Electron Devices*,

vol. 32, no. 3, pp. 691–699, Mar. 1985.

[31] W. Weber, C. Werner, and A. V. Schwerin, “Lifetimes and substrate currents in static and dynamic hot-carrier degradation,” in *1986 International Electron Devices Meeting*, 1986, pp. 390–393.

[32] Woltjer and Paulzen, “Universal description of hot-carrier-induced interface states in NMOSFETs,” in *International Technical Digest on Electron Devices Meeting*, 1992, pp. 535–538.

[33] Chen Ih-Chin, Choi Jeong Yeol, and Hu Chenming, “The effect of channel hot-carrier stressing on gate-oxide integrity in MOSFETs,” *IEEE Trans. Electron Devices*, vol. 35, no. 12, pp. 2253–2258, 1988.

[34] B. Eitan, D. Frohman□Bentchkowsky, and J. Shappir, “Impact ionization at very low voltages in silicon,” *J. Appl. Phys.*, vol. 53, no. 2, pp. 1244–1247, Feb. 1982.

[35] B. Ricco, E. Sangiorgi, and D. Cantarelli, “Low voltage hot-electron effects in short channel MOSFETs,” in *1984 International Electron Devices Meeting*, 1984, pp. 92–95.

[36] T. P. Ma and P. V. Dressendorfer, *Ionizing Radiation Effects in MOS Devices and Circuits*. 1989.

[37] P. J. McWhorter and P. S. Winokur, “Simple technique for separating the effects of interface traps and trapped-oxide charge in metal-oxide-semiconductor transistors,” *Appl. Phys. Lett.*, 1986.

[38] T. Tsuchiya and J. Frey, “Relationship between hot-electrons/Holes and degradation of p- and n-channel MOSFET’s,” *IEEE Electron Device Lett.*, vol. 6, no. 1, pp. 8–11, Jan. 1985.

[39] Y. Tsividis and C. McAndrew, *Operation and Modeling of the MOS Transistor, Third Edtion International Edition*. OUP USA, 2012.

[40] D. K. Schroder, *Semiconductor Material and Device Characterization*. Hoboken, NJ, USA: John Wiley & Sons, Inc., 2005.

[41] S. K. Lai, “Interface trap generation in silicon dioxide when electrons are captured by trapped holes,” *J. Appl. Phys.*, 1983.

[42] E. Takeda, T. Hagiwara, and A. Shimizu, “Role of Hot-Hole Injection in Hot-Carrier Effects and the Small Degraded Channel Region in MOSFET’S,” *IEEE Electron Device Lett.*, 1983.

[43] P. Heremans, R. Bellens, G. Groeseneken, and H. E. Maes, “Consistent model for the hot-carrier degradation in n-channel and p-channel MOSFETs,” *IEEE Trans. Electron Devices*, vol. 35, no. 12, pp. 2194–2209, 1988.

[44] D. Saha, D. Varghese, and S. Mahapatra, “Role of anode hole injection and

valence band hole tunneling on interface trap generation during hot carrier injection stress," *IEEE Electron Device Lett.*, 2006.

[45] E. Li, E. Rosenbaum, J. Tao, and P. Fang, "Projecting lifetime of deep submicron MOSFETs," *IEEE Trans. Electron Devices*, 2001.

[46] D. S. Ang, H. Liao, T. W. H. Phua, and C. H. Ling, "Evidence for a composite interface state generation mode in the CHE-stressed deep-submicrometer n-MOSFET," *IEEE Trans. Electron Devices*, 2004.

[47] D. S. Ang and C. H. Ling, "A reassessment of ac hot-carrier degradation in deep-submicrometer LDD N-MOSFET," *IEEE Electron Device Lett.*, vol. 24, no. 9, pp. 598–600, Sep. 2003.

[48] H. Kufluoglu, "MOSFET Degradation due to Negative Bias Temperature Instability (NBTI) and Hot Carrier Injection (HCI), and Its Implications for Reliability-Aware VLSI Design," Purdue University, 2007.

[49] F. C. Hsu and S. Tam, "Relationship Between MOSFET Degradation and Hot-Electron-Induced Interface-State Generation," *IEEE Electron Device Lett.*, 1984.

[50] K. Chain, J. Huang, J. Duster, P. K. Ko, and C. Hu, "A MOSFET electron mobility model of wide temperature range (77 - 400 K) for IC simulation," *Semicond. Sci. Technol.*, vol. 12, no. 4, p. 355, 1997.

[51] S. Cristoloveanu, H. Haddara, and N. Revil, "Defect localization induced by hot carrier injection in short-channel MOSFETs: Concept, modeling and characterization," *Microelectron. Reliab.*, 1993.

[52] H. Haddara and S. Cristoloveanu, "Profiling of stress induced interface states in short channel MOSFETs using a composite charge pumping technique," *Solid. State. Electron.*, vol. 29, no. 8, pp. 767–772, Aug. 1986.

[53] T. H. Ning and H. N. Yu, "Optically induced injection of hot electrons into SiO 2," *J. Appl. Phys.*, vol. 45, no. 12, pp. 5373–5378, Dec. 1974.

[54] R. J. Milanowski, M. P. Pagey, A. I. Matta, B. L. Bhuva, L. W. Massengill, and S. E. Kerns, "Combined Effect of X-Irradiation and Forming Gas Anneal on the Hot-Carrier Response of MOS Oxides," *IEEE Trans. Nucl. Sci.*, 1993.

[55] H. Haddara and G. Ghibaudo, "Analytical modeling of transfer admittance in small MOSFETs and application to interface state characterisation," *Solid State Electron.*, 1988.

[56] N. Balkan, *Hot electrons in semiconductors : physics and devices*. 1998.

[57] M. G. Ancona, N. S. Saks, and D. McCarthy, "Lateral distribution of hot-carrier-induced interface traps in MOSFETs," *IEEE Trans. Electron Devices*, vol. 35, no. 12, pp. 2221–2228, 1988.

[58] P. K. Ko, C. Hu, and S. Tam, “Lucky-Electron Model of Channel Hot-Electron Injection in MOSFET’s,” *IEEE Trans. Electron Devices*, 1984.

[59] T. H. Ning and R. R. Troutman, “Hot-Electron Emission in N-Channel IGFET’s,” *IEEE J. Solid-State Circuits*, 1979.

[60] E. Takeda and N. Suzuki, “An Empirical Model for Device Degradation Due to Hot-Carrier Injection,” *IEEE Electron Device Lett.*, 1983.

[61] W. Shockley, “Problems related to p-n junctions in silicon,” *Czechoslov. J. Phys.*, 1961.

[62] Shankar P. Sinha, “Hot-Carrier Reliability of Silicon-on-Insulator (SOI) MOSFETs and Applications to Non-Volatile Memories,” George Mason University, 1995.

[63] Y. Leblebici, “Modeling and simulation of hot-carrier induced device and circuit degradation for VLSI reliability,” University of Illinois, Urbana Champaign, 1991.

[64] P. Heremans, G. Van den Bosch, R. Bellens, G. Groeseneken, and H. E. Maes, “Temperature dependence of the channel hot-carrier degradation of n-channel MOSFET’s,” *IEEE Trans. Electron Devices*, vol. 37, no. 4, pp. 980–993, Apr. 1990.

[65] K. R. Mistr and B. Doyle, “AC versus DC Hot-Carrier Degradation in n-Channel MOSFETs,” *IEEE Trans. Electron Devices*, 1993.

[66] K. Yamaguchi, S. Asai, and M. Mock, “A Numerical Model of Avalanche Breakdown in MOSFET’s TORU TOY ABE,” *IEEE Trans. Electron Devices*, 1978.

[67] Fu-Chieh Hsu, Ping-Keung Ko, Simon Tam, Chenming Hu, and R. S. Muller, “An analytical breakdown model for short-channel MOSFET’s,” *IEEE Trans. Electron Devices*, vol. 29, no. 11, pp. 1735–1740, Nov. 1982.

[68] Fu-Chieh Hsu, R. S. Muller, and Chenming Hu, “A simplified model of short-channel MOSFET characteristics in the breakdown mode,” *IEEE Trans. Electron Devices*, vol. 30, no. 6, pp. 571–576, Jun. 1983.

[69] P. K. Ko, R. S. Muller, and C. Hu, “A unified model for hot-electron currents in MOSFET’s,” *1981 Int. Electron Devices Meet.*, 1981.

[70] T. Y. Chan, P. K. Ko, and C. Hu, “Dependence of channel electric field on device scaling,” *IEEE Electron Device Lett.*, vol. 6, no. 10, pp. 551–553, Oct. 1985.

[71] P. S. Winokur, J. R. Schwank, P. J. McWhorter, P. V. Dressendorfer, and D. C. Turpin, “Correlating the Radiation Response of MOS Capacitors and Transistors,” *IEEE Trans. Nucl. Sci.*, 1984.

[72] K. F. Galloway, C. L. Wilson, and L. C. Witte, “Charge-Sheet Model Fitting to

Extract Radiation-Induced Oxide and Interface Charge," *IEEE Trans. Nucl. Sci.*, vol. 32, no. 6, pp. 4461–4465, 1985.

[73] J. R. Brews, "A charge-sheet model of the MOSFET," *Solid State Electron.*, 1978.

[74] W. Wu, T. L. Chen, G. Gildenblat, and C. C. McAndrew, "Physics-based mathematical conditioning of he MOSFET surface potential equation," *IEEE Trans. Electron Devices*, 2004.

[75] I. S. Esqueda, "Modeling of Total Ionizing Dose Effects in Advanced Complementary Metal-Oxide-Semiconductor Technologies," Arizona State University, 2011.